Do environmental justice policies narrow inequality?*

Danae Hernandez-Cortes, Kyle Meng, Chris Timmins & Paige Weber

March 2025
PRELIMINARY DRAFT

Abstract

How does improving the local environment impact welfare inequality? This paper combines an equilibrium location sorting model with a novel reduced-form estimator of pollution's general equilibrium effects to quantify the welfare disparity consequences of demographically-targeted environmental policies. We apply this framework to recent years in Chicago, using data on individual migration histories and air pollution, an atmospheric transport model, and a research design leveraging local air pollution changes from remotely-determined natural gas supply shocks. Differentiating between effects on welfare and environmental exposure, we find that policies designed to narrow environmental inequality can actually widen it in some cases because of ensuing relocations. While we find that policies generally narrow welfare inequality, we find little variation between policies that do and do not have demographic targets, suggesting that sorting largely nullifies the policies' initial distributional intent.

*Hernandez-Cortes: School of Sustainability and School for the Future of Innovation in Society, Arizona State University, Danae.Hernandez-Cortes@asu.edu, Meng: Bren School and Dept. of Economics, UC Santa Barbara and NBER, kmeng@bren.ucsb.edu, Timmins: Real Estate and Urban Land Economics Department at the Wisconsin School of Business ctimmins@wisc.edu Weber: Energy and Resources Group, UC Berkeley, paigeweber@berkeley.edu. The authors have no financial or other conflicts of interest to disclose.

1 Introduction

A growing literature documents systematic disparities in pollution exposure by race, ethnicity, and socio-economic status.[1] Such pollution disparities have prompted calls for environmental justice policies—broadly, place-based policies that explicitly clean up locations where minoritized individuals reside. However, it remains unclear how such targeted place-based environmental policies impact welfare inequality between individuals from minoritized and other groups (Depro, Timmins and O'Neil, 2015; Banzhaf, Ma and Timmins, 2019; Wang, 2021).

The central mediating mechanism is residential sorting. Consider a policy that improves local air quality in a historically under-resourced location. Rosen (1974)'s canonical hedonic model describing the sorting of households according to amenities predicts higher housing prices in a place with improved air quality. Households in that location unable to bear such higher housing costs may have to move out, forgoing the environmental improvement. While households from elsewhere may move in because they are willing to pay for the environmental improvement. As such, a policy that aims to narrow an environmental disparity based on initial demographic characteristics has unclear consequences on welfare disparity after sorting.

The decision to move depends not only on the change in the local environment, but on ensuing changes in housing costs and other amenities locally and elsewhere. Recent empirical studies document an expanding set of local amenities affected by local and nearby air quality—for example, education, crime, recreation[2]— but do not link such impacts to welfare. A structural model of residential sorting with endogenous amenities would quantify welfare consequences.[3] But estimation requires separate identification strategies for the pref-

[1]These disparities are often referred to in the literature as an environmental justice gap (EJ gap). EJ gaps across many settings have been shown through case (Bullard, 2000; Bowen, 2002; Ringquist, 2005; Mohai, Pellow and Roberts, 2009*a*; Banzhaf, Ma and Timmins, 2019) and population-level (Tessum et al., 2019; Colmer et al., 2020; Currie, Voorheis and Walker, 2020) studies. See Cain et al. (2024) for a summary of recent economics oriented research in environmental justice, and Mohai, Pellow and Roberts (2009*b*) provides a summary of earlier EJ research prior to that.

[2]The following provide empirical documentation of indirect amenity effects of pollution on education: (Currie et al., 2009; Persico, Figlio and Roth, 2020; Liu and Salvo, 2018); crime: (Bondy, Roth and Sager, 2020; Herrnstadt and Muehlegger, 2015); and recreation (Liu, Hanley and Campbell, 2020; Liang et al., 2020).

[3]For an example of this approach, see Diamond (2017).

erences of each amenity, along with the assumption that all relevant amenities are accounted for structurally and observed empirically.

This paper develops a hybrid approach for quantifying changes in welfare dispersion among renter households following a demographically-targeted, place-based environmental policy. Our approach builds on a standard discrete location choice model (e.g., Bayer, Ferreira and McMillan (2007)) to facilitate a welfare interpretation. Within this model, we develop a novel reduced-form approach to flexibly estimate the impact of local and non-local environmental improvements on welfare due to both the environment improvement directly and its endogenous impacts on rental prices and other amenities. Importantly, we need not explicitly observe the full set of amenities affected by local and non-local environmental changes, nor recover amenity-specific preference parameters.

To demonstrate our approach, we study air quality improvements during the 2010s over the Chicago core-based statistical area (Chicago-Naperville-Elgin CBSA, Chicago CBSA thereafter). Our estimation combines data on individual migration histories and air pollution, an atmospheric transport model, and a research design leveraging air pollution changes from remotely-determined natural gas supply shocks. As counterfactuals, we consider policies that have the same aggregate air pollution improvement across the Chicago CBSA but with different spatial distributions according to initial demographic characteristics. We find that while these policies all narrow welfare inequality, there is little variation in these effects across alternative demographically-targeted policies, suggesting that sorting nullifies much of the policies' initial distributional aims. We also quantify how these policies alter the distribution of environmental exposure after sorting, showing that in some cases post-sorting environmental disparity widens even when policies narrow pre-sorting environmental disparity.

This paper contributes to the literature on hedonic housing market valuations, equilibrium sorting models used for policy analysis, and environmental justice. The existing literature has documented disparities in environmental amenities, finding that minoritized and low-income communities experience higher pollution on average (Tessum et al., 2021; Colmer et al., 2020; Currie, Voorheis and Walker, 2020). Some of the mechanisms behind these disparities are residential sorting (Depro, Timmins and O'Neil, 2015; Heblich,

Trew and Zylberberg, 2021; Bakkensen and Ma, 2020), discriminatory behavior or policies (Christensen, Sarmiento-Barbieri and Timmins, 2022; Christensen and Timmins, 2022), and information about pollution sources (Hausman and Stolper, 2021; Wang et al., 2021). We advance this literature by pairing a source of exogenous variation in local air quality with an equilibrium sorting model. Further, we develop a novel technique for flexibly accounting for endogenous amenities, that is, the indirect effects of changes in amenities on other amenities. Our model also captures spillovers of local amenity improvements to nearby locations. Our approach may be applied more broadly beyond environmental settings to evaluate the welfare consequences of other placed-based policies—industrial subsidies, infrastructure projects, housing subsidies—in the presence of sorting and endogenous amenities.

The rest of the paper proceeds as follows. Section 2 describes the model, Section 3 describes the data, Section 4 details the estimation method, Section 5 presents the results, and Section 6 concludes.

2 Theoretical framework

Section 2.1 presents the change in welfare inequality following a place-based environmnetal policy that targets baseline demographic characteristics. We also present alternative inequality metrics that are of interest or examined in prior literatures. Section 2.2 presents a discrete location choice model used to characterize equilibrium sorting outcomes. Section 2.3 presents a reduced-form approach to estimating general equilibrium effects of changes in air quality, which flexibly captures the indirect effects of local air quality improvements on other local amenities, as well as spillovers across space.

2.1 Measures of inequality

Let i index individuals by income ℓ and race/ethnicity r. Locations are indexed by j and there are two time periods $t = 0, 1$. Baseline air quality across locations is characterized by the vector $\mathbf{x}_0 = \{x_{10}, x_{20}, ...x_{j0}, ...\}$. The vector of air quality following a demographically-targeted, placed-based environmental policy is $\mathbf{x}_1 = \{x_{11}, x_{21}, ...x_{j1}, ...\}$. Consider, for example, the Black (b) - white (w) race-based welfare gap as the difference in expected welfare in

any one state. We are interested in the change in the welfare gap following the policy:

$$\Delta W_\ell = \Big(\underset{i\in\{\ell b\}}{E}[W_{ij}(\mathbf{x}_1)] - \underset{i\in\{\ell w\}}{E}[W_{ij}(\mathbf{x}_1)] \Big) - \Big(\underset{i\in\{\ell b\}}{E}[W_{ij}(\mathbf{x}_0)] - \underset{i\in\{\ell w\}}{E}[W_{ij}(\mathbf{x}_0)] \Big). \quad (1)$$

There are several aspects of equation (1) worth noting. First, expected welfare for individuals in a demographic group is a function of air quality across all locations. This is because changes in both local and remote air quality can induce residential sorting, which affects welfare through endogenous changes in housing costs and local amenities in all locations. Second, $\Delta W_\ell < 0$ and $\Delta W_\ell > 0$ implies a widening and narrowing of a race-based welfare gap, respectively, only when there is initial Black-white welfare inequality. Third, $\Delta W_\ell > 0$ may be sufficiently positive to result in a gap in the opposition direction.

To understand how sorting plays a roll in ΔW_ℓ, it is instructive to consider several other inequality metrics. The first is:

$$\Delta \widetilde{x}_\ell = \Big([x_{\ell b0}] - [x_{\ell w0}] \Big) - \Big([x_{\ell b1}] - [x_{\ell w1}] \Big), \quad (1')$$

where the elements $x_{\ell bt}$ and $x_{\ell wt}$ are per capita pollution metrics based on residential locations in $t = 0$ and pollution outcomes in $t = 1$. This metric represents the change in pollution exposure disparity under the baseline population distribution. This widely-used metric in the environmental justice and public health literatures assumes no re-sorting and focuses only on environmental exposure under baseline demographic patterns. A second metric that allows for sorting, but still focused on environmental exposure is:

$$\Delta x_\ell = \Big(\underset{i\in\{\ell b\}}{E}[\mathbf{x}_0] - \underset{i\in\{\ell w\}}{E}[\mathbf{x}_1] \Big) - \Big(\underset{i\in\{\ell b\}}{E}[\mathbf{x}_0] - \underset{i\in\{\ell w\}}{E}[\mathbf{x}_1] \Big), \quad (1'')$$

which quantities the gap in environmental exposure after accounting for relocation induced by the policy. While the outcome in this measure is still an environmental exposure, the expectation operator here is used to signal that households' environmental exposure depends on their location choice, which depends on characteristics of all locations. Finally, one can

also construct:

$$\Delta\widetilde{W}_\ell = \Big(\underset{i\in\{\ell b\}}{E}[W_{ij}(x_{j1})] - \underset{i\in\{\ell w\}}{E}[W_{ij}(x_{j1})]\Big) - \Big(\underset{i\in\{\ell b\}}{E}[W_{ij}(x_{j0})] - \underset{i\in\{\ell w\}}{E}[W_{ij}(x_{j0})]\Big) \quad (1''')$$

which incorporates the value of local air quality changes on local housing costs and amenities but assumes individuals do not move as a consequence. This eliminates potential changes in local amenities and non-local housing costs and amenities.

Our primary aim is to estimate ΔW_ℓ, the change in the welfare gap inclusive of sorting and endogenous amenities. As a point of comparison, we will also report alternative metrics, notably $\Delta\widetilde{x}_\ell$ and Δx_ℓ to understand the role of sorting and valuation in our main result. We do not estimate $\Delta\widetilde{W}_\ell$ as doing so requires hedonic estimates of the marginal willingness to pay for air quality by race, ethnicity and income, which are not available and in practice very difficult to obtain.

2.2 Sorting Model

Estimating equation (1) under an air quality change requires more structure. A natural point of departure is to specify a discrete choice sorting model. Households choose a location j^* at each time t to maximize utility U_{ijt} among J locations.[4] That is, each renter's location choice satisfies the following:

$$\begin{aligned} j^* &= argmax_{j\in J}\{U_{ijt}\} \\ U_{ijt} &= V_{ijt} + \epsilon_{ijt} \\ V_{ijt} &= \zeta^{\ell r} m_{it} + \underbrace{\alpha^\ell p_{jt} + \rho^{\ell r} x_{jt} + \nu^{\ell r} Q_{jt} + \gamma_j^{\ell r} + \mu_t^{\ell r}}_{\delta_{jt}^{\ell r}}. \end{aligned} \quad (2)$$

m_{it} is an individual level indicator variable that equals 1 for any tracts in t that the renter

[4]This paper is focused on renters, and we leave the plausibly dynamic decision problem of owner households, who make location decisions that involve future housing value, to future work. Table A1 shows that the percentage of renters who moved in the 2010-2018 period is 27.4% nationally and 30.8% in the Chicago CBSA, while the percentage of owners who moved is 7.1% and 7.9% nationally and in the Chicago CBSA, respectively.

was not located in $t-1$ such that $\zeta^{\ell r}$ captures the income-race/ethnicity-specific utility cost of moving. Annual rental price in location j is p_{jt} so that α^{ℓ} is the income-specific marginal utility of income. The parameter $\rho^{\ell r}$ represents preferences for air quality which we allow to vary by income and race/ethnicity, though it need not do so empirically, and the marginal willingness to pay for air quality is $\frac{\rho^{\ell r}}{\alpha^{\ell}}$. Q_{jt} is a vector of local amenities—public schools, public safety, retail options, homophily—with preferences $\nu^{\ell r}$ that could vary by income and race/ethnicity. Importantly, as noted above, some amenities in Q_{jt} are endogenous to both local and remote air quality and may even be unobserved. We address both issues in Section 2.3. The parameters $\gamma_j^{\ell r}$ and $\mu_t^{\ell r}$ denote location and year-specific determinants of utility, respectively, which we also allow to vary by income and race/ethnicity. Collectively, we denote these location-time components of utility as $\delta_{jt}^{\ell r}$. Lastly, we assume the unobserved term ϵ_{ijt} is drawn from an extreme value type-1 distribution.

Our sorting model embeds several assumptions. First, renters are myopic and make annual location choices, motivated in part by the prevalence of yearlong rental leases. This modeling choice, together with our subsequent estimation approach, requires that utilities re-equilibrate to air quality changes annually. We relax this assumption in Appendix E where we estimate a long-difference version of the model and generate corresponding results, which are qualitatively similar to the results in our annual model. Second, renters make choices based on the characteristics of all locations in that year, which requires renters to have rational expectations about the characteristics of the location in year t.[5] Finally, we assume that individual moving costs are the same regardless of origin and destination locations. This assumption may be implausible when relocation occurs across large geographies such as counties or states for which moving costs vary. For our empirical setting, where renters choose among census tracts in a metropolitan area, this assumption may be reasonable.

Under these assumptions, Train (2009) shows that the change in the welfare gap in equation (1) can be written as:

[5]This implies that renters deciding where to live in 2011 have rational expectations about average annual air quality in 2011. Interannual changes in air quality would be included in utility when they are correlated with the overall average annual air quality. The related dimensions of annual air quality variation are discussed in Section 4.2 and Appendix B.

$$\Delta W_\ell = \frac{1}{\alpha^\ell}\left[\left(ln\Big(\Sigma_{j=1}^{J} exp\big\{\widehat{V}_{j\ell b}(\mathbf{x_1})\big\}\Big) - ln\Big(\Sigma_{j=1}^{J} exp\big\{\widehat{V}_{j\ell w}(\mathbf{x_1})\big\}\Big)\right) - \left(ln\Big(\Sigma_{j=1}^{J} exp\big\{\widehat{V}_{j\ell b}(\mathbf{x_0})\big\}\Big) - ln\Big(\Sigma_{j=1}^{J} exp\big\{\widehat{V}_{j\ell w}(\mathbf{x_0})\big\}\Big)\right)\right]. \quad (3)$$

$\widehat{V}_{j\ell r}(\cdot)$ indicates estimated utilities detailed below. The term $\frac{1}{\alpha^\ell}$ makes clear that this gap is specific to a given income group. Thus, we can use estimates of $\widehat{V}_{j\ell r}(\cdot)$ across race/ethnicity and time to recover the direction of the change in the gap in a given income group. And this can be done without estimating marginal utility of incomes, α^ℓ. While we will not be able to recover the ultimate size of the gap, we will be able to recover the direction of change induced by the policy, which is sufficient for our research question.

2.3 Reduced-form representation

Estimating equation (2) is challenging beyond the typical difficulty of obtaining exogenous variation in air quality x_{jt}. First, local housing costs and amenities are endogenous to local air quality, as documented widely in the empirical literature.[6] But this dependence is not merely local, as a location's housing costs and amenities are also affected by air quality elsewhere through equilibrium sorting.[7] Finally, not all amenities that respond to local and remote air quality may be observed, presenting a direct measurement challenge.

To jointly address these challenges, we embed our logit model with a reduced-form representation of all the direct and indirect effects of local and non-local air quality.[8] From equation (2), we have that $\delta_{jt}^{\ell r}$ is a function of housing costs, p_{jt}, and (both observed and

[6]The following provide empirical documentation of indirect amenity effects of pollution on education: (Currie et al., 2009; Persico, Figlio and Roth, 2020; Liu and Salvo, 2018); crime: (Bondy, Roth and Sager, 2020; Herrnstadt and Muehlegger, 2015); and recreation (Liu, Hanley and Campbell, 2020; Liang et al., 2020).

[7]This spatial effect can manifest also through how local public goods are financed or simply through access via travel. For example, a higher quality school increases the location utility not only of the census tract the school is located in, but also in nearby tracts for households that have that school in their choice set. Likewise, an outdoor park benefits nearby households that travel to access it.

[8]While we have not seen this approach used in other sorting models to handle endogenous amenities, a related technique is used in a working paper by Berry and Haile (2024) to address endogeneity in voting choices.

unobserved) amenities, Q_{jt}. Suppose we can decompose these variables into functions of local and non-local exogenous air quality:

$$p_{jt} = \kappa_{P0} x_{jt} + \kappa_{P1} z_{jt} + \zeta_{Pjt} \tag{4}$$

$$Q_{jt} = \kappa_{Q0} x_{jt} + \kappa_{Q1} z_{jt} + \zeta_{Qjt}. \tag{5}$$

z_{jt} denotes a set of air qualities at different distance bands from census tract j.[9] ζ_{Pjt} and ζ_{Qjt} are error terms. Inserting Equations (4) and (5) into $\delta_{jt}^{\ell r}$ in Equation (2) yields:

$$\delta_{jt}^{\ell r} = \underbrace{\left(\alpha^{\ell} \kappa_{P0} + \rho^{\ell r} + \nu^{\ell r} \kappa_{Q0}\right)}_{\beta_0^{\ell r}} x_{jt} + \underbrace{\left(\alpha^{\ell} \kappa_{P1} + \nu^{\ell r} \kappa_{q1}\right)}_{\beta_1^{\ell r}} z_{jt} + \gamma_j + \mu_t + \underbrace{\alpha^0 \zeta_{Pjt} + \nu^{\ell r} \zeta_{jt} + \xi_{jt}}_{\text{error}}, \tag{6}$$

where $\beta_0^{\ell r}$ captures the total effect of local air quality on utility for a given income-race/ethnicity, inclusive of direct and indirect effects through housing costs and all endogenous amenities. Similarly, $\beta_1^{\ell r}$ captures the total direct and indirect effect of non-local air quality. The key to this reduced-form representation is that it sidesteps the need to separately estimate each preference parameter (i.e., α^{ℓ}, $\rho^{\ell r}$, $\nu^{\ell r}$) and how local and non-local air quality affects prices and amenities (i.e., κ_*). It also does not require observing all relevant amenities. While this approach allows for estimation of welfare gap changes, it is unable to unpack the determinants of those welfare effects. However, as validation, we do estimate equation (4) and equation (5) for observed amenities to document that air quality does have effects in our empirical setting that is document elsewhere, with results provided in Table A5.

3 Data

This section discusses the data used to estimate both the residential sorting model and plausibly exogenous changes in air quality due to fracking. Data discussed in Sections 3.1

[9] Specifically, $z_{jt} = \{x_{kt}^1, ..., x_{kt}^n\}$, where x_{jk}^n denotes the air quality n distance away from tract j. The construction of these terms for estimation is discussed in 4.2.

and are used to estimate the sorting model, with supplementary data in Section 3.2; and data discussed in Sections 3.3, 3.4, and 3.5 are used to estimate air quality changes driven by fracking.

3.1 Residential location data

We use the proprietary dataset InfoUSA Residential Historical Data Set from Data Axle (hereafter Data Axle) to observe household location decisions over time as well as household characteristics. These panel data are unique at the household–year level, allowing us to observe year to year bilateral migration decisions. Data Axle provides the household latitude and longitude, which we use to find the household's census tract of residence. We also use Data Axle's imputed inputs for household income, race, ethnicity, and status as renter or owner. We use the income variable to classify households into quartiles of income types, with renters with income below the 25th percentile of income in the renter panel coded as income type 1, and renters with income above or equal to the 75th percentile of income coded as income type 4.

3.2 U.S. demographics, income, and rental prices

We use U.S. demographic, income, and rental data from the American Community Survey 5-year estimates (ACS 5-yr) for several supporting analyses. For the purposes of descriptive regressions and statistics, we use (real) rent prices from the ACS 5-yr, where we use each 5-year estimate as the rent price for the midyear, i.e., ACS 2009–2013 is used for rent prices in 2011. We match average rent values to migration data based on census tract identifiers. Table 1 panel (a) shows the average rent values alongside other demographics for the national average (column 1) and the Chicago CBSA (column 2) for our study period, 2011–2018.

3.3 Electricity generating units data

We obtain data on electricity production and emissions (NO_x, SO_2) from the Clean Air Markets Division of the U.S. Environmental Protection Agency, which collects information on hourly data for electricity generating units over 25MW in capacity. We use these data

Table 1: Descriptive statistics (census and Data Axle)

	(1)	(2)
	All census tracts	Chicago CBSA census tracts
Real rent	1038.584	1134.675
	(434.97)	(365.87)
Hispanic percent	0.167	0.205
	(0.23)	(0.24)
Black percent	0.133	0.214
	(0.22)	(0.33)
White percent	0.644	0.523
	(0.31)	(0.33)
Other minority percent	0.056	0.058
	(0.10)	(0.08)
Real median income	46289.506	47027.583
	(33404.30)	(36533.73)
Poverty percent	0.164	0.157
	(0.13)	(0.13)
Observations	586,495	13,219

NOTES: Descriptive statistics for the 2011–2018 period, nationally and for the Chicago CBSA. Panel (a) shows data from census obtained via IPUMS.

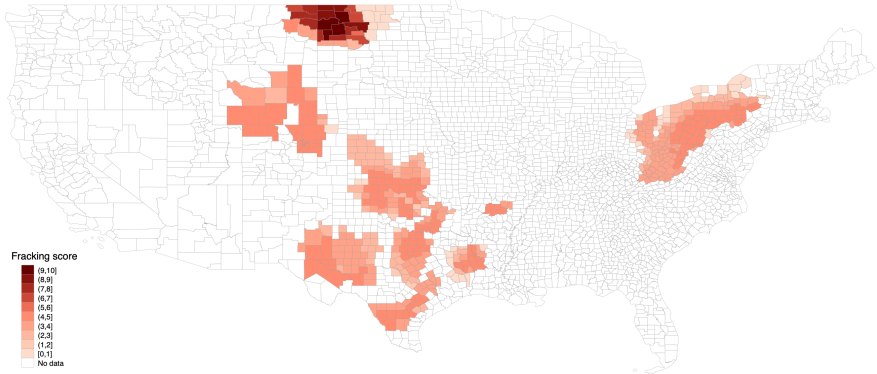
to obtain annual emissions levels by electricity generating unit. We also use geographic information on units as well as smoke stack characteristics (height, velocity, temperature, and diameter) from the EIA Form-860 to model pollution dispersion. We follow the methods in Hernandez-Cortes, Meng and Weber (2023) to merge and process the electricity generating units data for use in the pollution dispersal model.

3.4 Shale gas propensity and natural gas pipelines

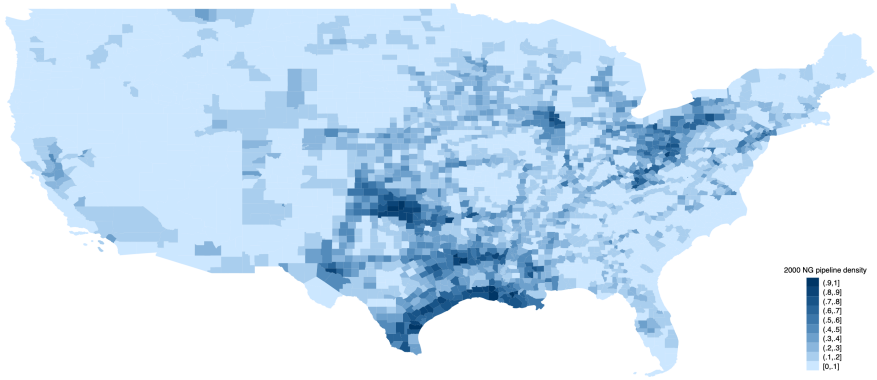
In Section 4.2 we present an instrumental variable approach for changes in ambient air quality. While the details of the identification argument are presented there, this section reviews the data used to construct the instrument. We use a measure of county-level fracking prospectivity score, which is used in Bartik et al. (2019) and originally constructed by Rystad Energy, a proprietary data provider. The score is developed to measure the potential productivity of different geographies using geological factors that determine fracking potential. Because there are multiple shale plays in a county, we follow Bartik et al. (2019) and take maximum prospect score across all shale plays under a county. The county-level values

Figure 1: Maps of fracking propensity and natural gas pipeline density

(a) County-level prospect fracking score



(b) County-level 2000 natural gas pipeline density



NOTES: Panel (a) shows the county-level measure of shale gas propensity by fracking score, which constitutes variable (R_i) discussed in Section 4.2. Panel (b) shows the natural gas pipeline density by county across the contiguous U.S. and constitutes variable (G_i) discussed in Section 4.2.

of this score are mapped in panel (a) of Figure 1.[10]

The next data input for our instrument is the pre-shale network of natural gas pipelines. We use these data to connect shale gas propensity to changes in electricity production, as the degree to which a generator is impacted by fracking will depend on their proximity—in pipeline distance—to fracked gas. We use pipeline infrastructure data from the EIA's U.S. Energy Atlas and calculate the density of natural gas pipelines as pipeline area divided by county area. Panel (b) of Figure 1 shows the (normalized) share of county area with natural gas pipelines using the pipeline network in 2000, before the introduction of fracking.

[10]Note that the geological factors that are inputs to the scores, as well as the functional forms, differ across shale plays so scores should not be compared across shale plays, but rather provide measures of county variation in fracking propensity within shale plays.

3.5 Air pollution data

For measures of ambient $PM_{2.5}$ concentrations in the U.S., we use Van Donkelaar et al. (2021)'s satellite-based estimates. Appendix B includes more information about this data product, including comparing $PM_{2.5}$ changes in our study period in the Van Donkelaar et al. (2021) data to changes observed in EPA monitors in the Chicago CBSA in Figure A5 and Figure A7. In other parts of our analysis, we compute $PM_{2.5}$ contributions just from electricity generating units. To do this, we use a pollution transport model, InMAP. InMAP models pollution transport based on electricity generating smoke stack unit characteristics and atmospheric and weather patterns developed by Tessum, Hill and Marshall (2017). We use InMAP's source-receptor matrix following Goodkind et al. (2019) to estimate how emissions from electricity generating units contribute to concentrations of $PM_{2.5}$ across a geographic grid of the contiguous U.S.. We then layer this spatial grid of pollution estimates onto U.S. census tracts to merge our $PM_{2.5}$ estimates with household location choices defined at the census tract level. This approach follows the procedure described in more detail in Hernandez-Cortes, Meng and Weber (2023). To illustrate the impact of pollution transport, Figure A4 shows the tract-level variation in $PM_{2.5}$ concentrations that results from emissions from a sample coal unit in the Chicago CBSA.

4 Estimation

The following section discusses the estimation procedure, broadly grouped in two areas. Section 4.1 discusses the estimation of the parameters of the equilibrium sorting model. Section 4.2 discusses the estimation of the coefficients in equation (6), capturing the general equilibrium effects of air quality on utility.

4.1 Estimating parameters of the sorting model

The estimation of the parameters of the sorting model proceeds in two steps. First, a BLP-contraction algorithm is used to recover an estimate of the unobserved location-time-income type-specific utilities, $\widehat{\delta_{jt}^{\ell r}}$ (Berry, Levinsohn and Pakes, 1995). Second, a nested

likelihood maximization algorithm is used to estimate the unknown parameters for moving costs. Details are provided below, where a will denote the iteration with respect to calculating the baseline utilities ($\delta_{jt}^{\ell r}$), and q will denote the iteration with respect to calculating the remaining parameters.

Step (1). This step is a contraction mapping to recover unobserved utilities, $\delta_{jt}^{\ell r}$, given an initial guess of moving costs, $\zeta^{\ell r}$. Assuming that ϵ_{ijt} are distributed i.i.d. Type I Extreme Value and given an initial guess for the parameters $\{\zeta^{\ell r,q}\}$ and baseline utilities ($\{\delta_j^{\ell r,a,q}\}_{j=1}^J$), the probability that renter household i of income group ℓ and race/ethnicity r chooses location j at time t is given by:

$$\pi_{ijt}^{a,q} = \frac{exp\{\delta_{jt}^{\ell r,a,q} + \zeta^{\ell r} m_{it}\}}{\Sigma_{j=1}^J \left[exp\{\delta_{jt}^{\ell r,a,q} + \zeta^{\ell r} m_{it}\}\right]} \tag{7}$$

From equation (7), the share of renters of income group ℓ living in location j at time t is given by:

$$\hat{\sigma}^{\ell r,a,q} = \frac{1}{N^{\ell r}} \sum_{i=1}^{N^{\ell r}} \pi_{ijt}^{a,q}, \tag{8}$$

where N corresponds to the number of individuals in group ℓr. Berry (1994) proves that the following iteration procedure will converge to the vector of $\delta_{jt}^{\ell r}$'s that equate observed to predicted shares, $\{\delta_{jt}^{\ell r*,q}\}_{j=1}^J$ given the parameter vector ($\zeta^{\ell r,q}$):

$$\delta_{jt}^{\ell r,a+1,q} = \delta_{jt}^{\ell r,a,q} + (ln\ \sigma_{jt}^{\ell r} - ln\ \hat{\sigma}_{jt}^{\ell r,a,q}), \tag{9}$$

where $\sigma_{jt}^{\ell r}$ denotes the observed share of individuals of income-race/ethnicity ℓr living in location j at time t. This procedure requires that one of the location-time-income-race/ethnicity baseline utilities is normalized. We do this by setting $\delta_{j=1,t}^{\ell r} = 0$, where $j = 1$ corresponds to the outside option. This normalization will allow us to estimate the expected welfare changes in equation 1, which compares welfare changes across race/ethnic groups, but not across income types.

Step (2). In this step, step (1) is nested inside a likelihood maximization algorithm. Given the parameter vector ($\zeta^{\ell r,q}$) and the corresponding vector of baseline utilities ($\{\delta_{jt}^{\ell r*,q}\}_{j=1}^{J}$) that equate predicted to actual shares, we calculate the likelihood of the observed data:

$$L(\delta_{jt}^{\ell r*,q}\zeta^{\ell r,q}|\sigma_{jt}^{\ell r}) = \Pi_{t=1}^{T}\Pi_{n=1}^{N^{\ell r}}\Pi_{j=1}^{J}\left[\pi_{ijt}^{*,q}\right]^{Y_{ijt}}, \tag{10}$$

where $Y_{ijt} = 1$ if renter i chooses j and $= 0$ otherwise. The maximization routine determines new values of ($\zeta^{\ell r,a}$) along with the corresponding values of $\left\{\delta_{jt}^{\ell r*,q+1}\right\}_{j=1}^{J}$ to increase the likelihood expression until it is maximized as: $\{\zeta^{\ell r*}\{\delta_{jt}^{\ell r*}\}_{j=1}^{J}\}$. Once $\{\delta_{jt}^{\ell r*}\}_{j=1}^{J}$ is recovered, the next step is to regress these estimated objects on exogenous changes to air quality, discussed below.

4.2 Identification of air quality impacts on utility

Overview of approach. This section discusses our approach to causally identify the impact of cleaner air on a location's utility. Our approach is motivated by the fact that variation in air quality is potentially correlated with unobserved factors impacting utility. Specifically, x_{jt} and z_{jt} in equation (6) may be correlated with the error term. To address this, we leverage a plausibly exogenous source of variation in air quality—changes in air quality from the advent of horizontal drilling and hydraulic fracturing to access natural gas. Fracking also led to a number of local amenity impacts for the communities near fracked wells, some of which are empirically documented in Bartik et al. (2019) and Jacobsen (2019). Our empirical strategy does not make any assumptions that are inconsistent with this empirical finding.

While horizontal drilling and hydraulic fracking as (separate) techniques to access oil and gas have been around for many years, their use together to access crude oil and natural gas in the U.S. started growing in the early 2000s, taking off by the end of the decade. By October 2011, well footage drilled by these new techniques in the U.S. had surpassed all other drilling approaches. These techniques involve drilling a well first vertically, and then extending it horizontally. The fracturing part comes after the well is drilled. In this step a liquid under high pressure is forced against a rock formation until it fractures. The fluid,

which contains small, solid particles, expands the fractures, allowing crude oil or gas to be accessed more easily (U.S. EIA, 2018). Though these techniques, which we will collectively refer to as fracking, are more expensive in terms of capital costs compared to conventional drilling techniques, their impact on increasing supply of crude oil and natural gas has ultimately decreased the prices of these energy sources. The decrease in the the price of natural gas reduced the cost natural gas generated electricity (Hausman and Kellogg, 2015). As a result, electricity generation from coal generating units fell while electricity from natural gas generating units increased, with natural gas surpassing coal electricity generation in the U.S. in 2016 (U.S. EIA, 2017). Since natural gas generated electricity is less pollution intensive, fracking resulted in improvements in air quality. The level of air quality improvement will vary spatially, based on the spatial distribution of gas and coal plants and which generators have access to fracked-gas. We will use this feature of the empirical setting to improve the relevance of our instrument, bringing in the density of the U.S. natural gas pipeline network.

In general, changes in air quality attributed to the electricity sector are a function of both changes in emissions from electricity generating units—e.g. sources of pollution—and the wind patterns connecting those emissions changes to households receiving the pollution—e.g. receptors of pollution. We use the InMAP source receptor matrix to estimate the impact of emissions from electricity generating units on concentrations of pollution at receptor locations. InMAP is a model of pollution transport and thus includes measurement error. For example, its model of pollution transport uses average annual wind speeds as of year 2005, which means averages of seasonal trends in wind and may be outdated to the extent that average annual wind speeds and directions have changed in our study period. Our estimation is at the annual level, so averaging over seasonal outcomes is not a problem.

To the extent that wind speeds and directions have changed in the period 2011—2018 compared to 2005, that would introduce additional measurement error in the construction of our instrument. However, that error is unlikely to violate our exclusion restriction. It would present a problem for our exclusion restriction if changes in wind speed and direction created tract-by-year changes in pollution that were correlated with tract-by-year components of the error term in equation 6. Given changes in wind are due to weather and climate related factors, this is unlikely to be the case.

Below we discuss in detail our identification strategy to construct instruments for (x_{jt}, z_{jt}) that are uncorrelated with the error term in equation (6). We first construct fracking-induced predicted emissions from electricity generating units. The predicted emissions leverage the exogenous variation in shale gas prospect scores across counties in the U.S. The predictions are improved, e.g. relevance of the instrument increased, by incorporating natural gas pipeline density in the U.S. in the year 2000, i.e. before the widespread use of fracking techniques. Then, we use a pollution dispersal model to convert these predicted emission changes to predicted changes in air quality.

Isolating exogenous changes in emissions from generating units. In this estimation task, we isolate the changes in electricity generating unit (EGU) emissions that are due to exogenous variation in the spatial distribution of shale gas supply, modulated by pipeline density. Following Bartik et al. (2019), denote R_i as the fracking prospect score for county i, which is constructed using geological factors that determine fracking potential. Because there are multiple shale plays in a county, we follow Bartik et al. (2019) and take maximum prospect score across all shale plays under a county.[11] The availability of shale natural gas should affect electricity output in counties not overlying a shale play. The degree those counties are affected by shale gas exploration depends on the pre-shale network of natural gas pipelines.[12] Denote county-level natural gas pipeline density in 2000 as G_i.

For each EGU g in county i, we define potential fracking supply as $S_g = R_g * G_i$ where R_g is the prospective fracking score for the nearest county j to EGU g by Euclidean distance with a positive prospective fracking score, or $R_g = R_{i^*}$ where $i^* = min_{i \in R_i > 0} |g - i|$. Panel (a) of Figure A8 shows S_g for every EGU that operated between 2000–2018. Note that S_g jointly weights proximity to a natural gas shale play and pre-fracking natural gas pipeline availability. For example, whereas Ohio and South Dakota are similarly close to natural gas plays (the Marcellus and Bakken, respectively), the greater density of natural gas pipelines in 2000 in Ohio generates a higher potential fracking supply than in South Dakota. This is consistent with observed changes in natural gas input prices for natural gas EGUs from EIA Form-923 data. As panel (b) of Figure A8 shows, the 2008–2018 drop in natural gas input

[11] The county-level values for R_i is mapped in panel (a) of Figure 1.

[12] Panel (b) of Figure 1 shows the (normalized) share of county area with natural gas pipelines using the pipeline network in 2000, before the introduction of fracking.

prices is much larger near the Marcellus formation than near the Bakken formation.

Next, define h_{gt} as an event time variable whereby the value zero indicates the last year before fracking began in nearest county i^*. Let E^p_{gt} denote emissions of primary pollutant $p \in \{NO_x, SO_2, PM_{2.5}\}$ from EGU g in year t. Further let each EGU g be characterized by fossil fuel $f \in \{coal, gas, oil\}$. We estimate the following event-study regression specification:

$$\begin{aligned} asinh(E^p_{gt}) = &\sum_{\substack{-4 \leq \tau \leq 10 \\ \tau \neq 0}} \kappa^{\text{gas}}_{p,\tau}[\mathbf{1}(\tau = h_{gt}) \times \mathbf{1}(f = \text{gas}) \times S_g] + \\ &\sum_{\substack{-4 \leq \tau \leq 10 \\ \tau \neq 0}} \kappa^{\text{coal}}_{p,\tau}[\mathbf{1}(\tau = h_{gt}) \times \mathbf{1}(f = \text{coal}) \times S_g] + \psi_g + \vartheta_{ot} + \nu^p_{gt} \end{aligned}$$

where ψ_g are EGU-level fixed effects. The vector of dummy variables ϑ_{ot} includes power plant-by-year and event time fixed effects. The error term ν^p_{gt} is clustered at the county level to account for arbitrary forms of heteroskedascity for EGUs within a county and serial correlation within an EGU over time. Our coefficients of interest are $\kappa^{\text{gas}}_{p,\tau}$ and $\kappa^{\text{coal}}_{p,\tau}$. When event time $\tau > 0$, this coefficient indicates the annual percentage point change in pollutant p emissions for coal and natural gas EGUs relative to oil EGUs after fracking becomes locally available. The coefficients when event time $\tau < 0$ provide an indirect test for pre-trends. Figure 2 plots estimates of coefficients $\kappa^{\text{gas}}_{p,\tau}$ (left panel) and $\kappa^{\text{coal}}_{p,\tau}$ (right panel) for each of the three primary pollutants (down rows).

Equation (11) is the fully-flexible event study specification. Guided by the functional form shown in Figure 2, we further estimate a more parsimonious version using a linear trend break model. Specifically, we estimate:

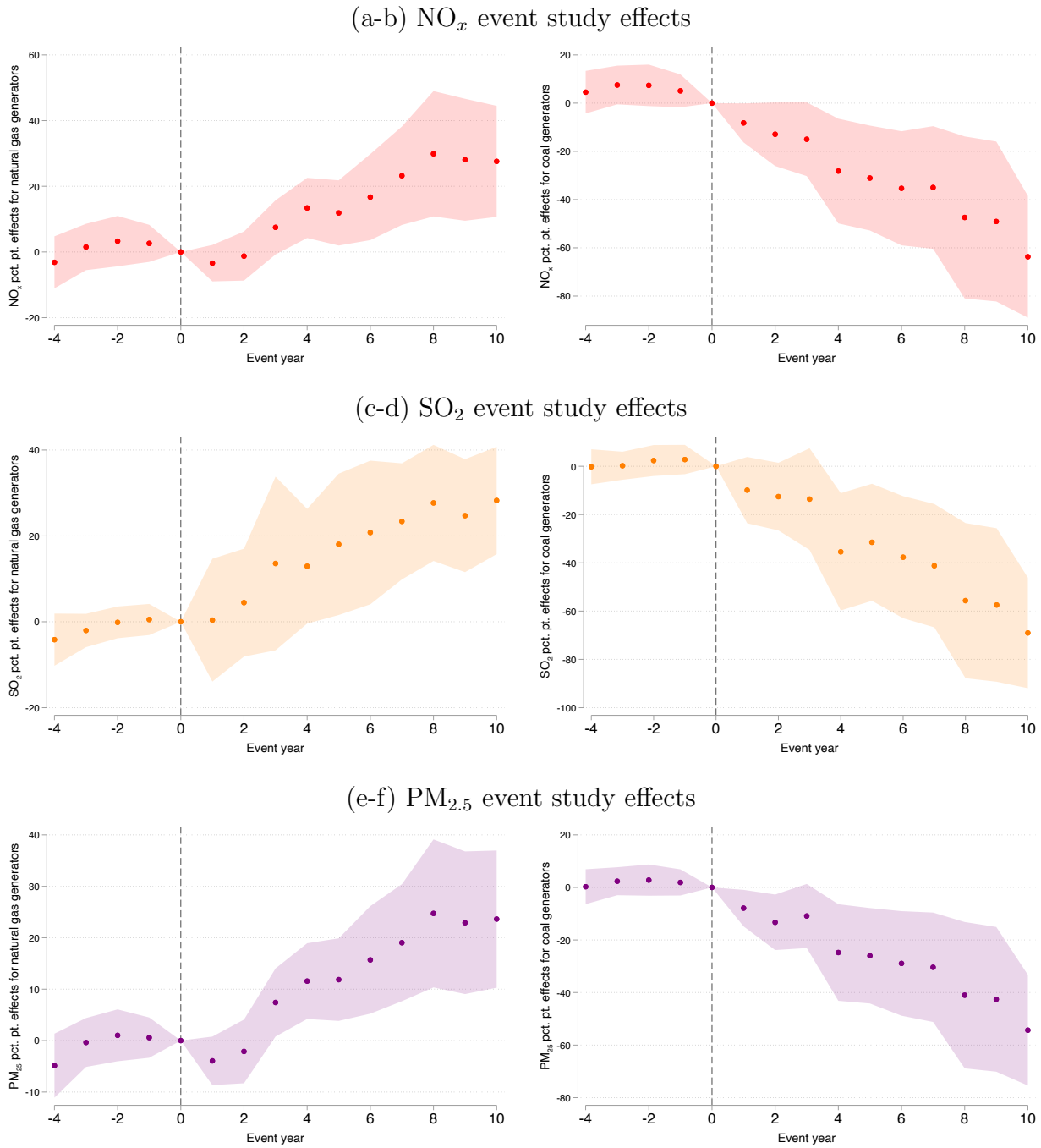
$$\begin{aligned} asinh(E^{pgt}) = &\beta^{\text{gas}}_{p,1}[h_{gt} \times \mathbf{1}(f = \text{gas}) \times S_g] + \beta^{\text{gas}}_{p,2}[h_{gt} \times \mathbf{1}(h_{gt} > 0) \times \mathbf{1}(f = \text{gas}) \times S_g] + \\ &\beta^{\text{gas}}_{p,3}[\mathbf{1}(h_{gt} > 0) \times \mathbf{1}(f = \text{gas}) \times S_g] + \\ &\beta^{\text{gas}}_{p,1}[h_{gt} \times \mathbf{1}(f = \text{gas}) \times S_g] + \beta^{\text{gas}}_{p,2}[h_{gt} \times \mathbf{1}(h_{gt} > 0) \times \mathbf{1}(f = \text{gas}) \times S_g] + \\ &\beta^{\text{gas}}_{p,3}[\mathbf{1}(h_{gt} > 0) \times \mathbf{1}(f = \text{gas}) \times S_g] + \\ &\psi_g + \vartheta_{ot} + \nu_{pgt}, \end{aligned}$$

where our parameter of interests are now $\beta_{p,2}^{\text{gas}}$ and $\beta_{p,2}^{\text{coal}}$, which test whether emissions of pollutant p for natural gas and coal EGUs exhibit trend breaks after the introduction of local fracking. Table A2 shows that there are statistically significant trend breaks.

For each EGU, we generate predicted emission changes $\Delta\widehat{E}_{gt}^{p}$ due to the introduction of fracking. Specifically, letting E_g^{op} denote the observed emissions of pollutant p when event time is zero, $\Delta\widehat{E}_{gt}^{p} = E_g^{op}[\widehat{\beta}_{p,2}^{\text{gas}} * h_{gt} * S_g + \widehat{\beta}_{p,3}^{\text{gas}} + 1]$ for a gas EGU and $\Delta\widehat{E}_{gt}^{p} = E_g^{op}[\widehat{\beta}_{p,2}^{\text{coal}} * h_{gt} * S_g + \widehat{\beta}_{p,3}^{\text{coal}} + 1]$ for a coal EGU. Predicted emissions change may exceed the maximum within sample emissions for a given EGU. To avoid this over- or under-prediction, we replace $\Delta\widehat{E}_{gt}^{p}$ if its absolute value exceeds that of the maximum observed sample emissions value for that EGU. Panel (a) of Figure 3 plots 2011–2018 NO_x predicted emissions for coal EGUs. As a comparison, panel (b) of Figure 3 shows the observed NO_x change from coal EGUs during 2011–2018. Panels (c) and (d) of Figure 3 shows predicted and observed NO_x changes for natural gas EGUs. The mechanism generating these results is that shale gas propensity modulated by pipeline availability provides access to natural gas. For this to be true, gas EGUs with a large S_g would also have lower natural gas prices. We study this by generating the same event study figure with natural gas prices from EIA-923 as the outcome. Figure A3 which shows suggestive evidence of lower generator-level natural gas prices following the event year.

Converting emissions to air quality. In this estimation step we convert predicted EGU-level emissions generated from the procedure above, $\Delta\widehat{E}^{p}gt$, to total $PM_{2.5}$ concentrations for a census tract j, $\Delta\widehat{X}_{jt}$, which equals $\sum_p \sum_g w_{gj}^{p} \Delta\widehat{E}_{gt}^{p}$, where w_{gj}^{p} are elements from the InMAP source-receptor matrix converting emissions of pollutant p from generator g to census tract j. Figure 3 shows the 2011–2018 total predicted $PM_{2.5}$, $\Delta\widehat{X}_{jt}$. Our predicted $PM_{2.5}$ concentrations show declines in the lower Midwest and the Southeast and also in the upper Midwest. Figure 3 shows that there is not much observed coal decline in the upper Midwest and thus electricity may not have played a role in the clean up of the upper Midwest. This analysis motivates our choice of the Chicago CBSA as our empirical setting for our study of location choice—a CBSA with among the most variation in air pollution explained by fracking. Because the variation is due to plausibly exogenous factors, choosing Chicago to study should not introduce selection bias. Rather, we focus on the Chicago CBSA

Figure 2: Effects of fracking on emissions and pollution from the electricity sector

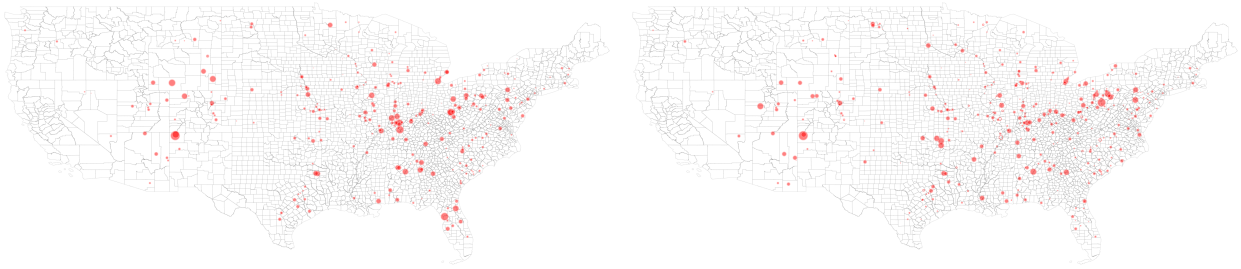


NOTES: These figures plot the estimates from event study regression in equation (11), with alternative dependent variables—NO$_x$, SO$_2$, and PM$_{2.5}$. The figures in the left column—(a), (c), (e)—show the impacts among natural gas generators. The figures in the right column—(b), (d), (f)—show the impacts among coal generators.

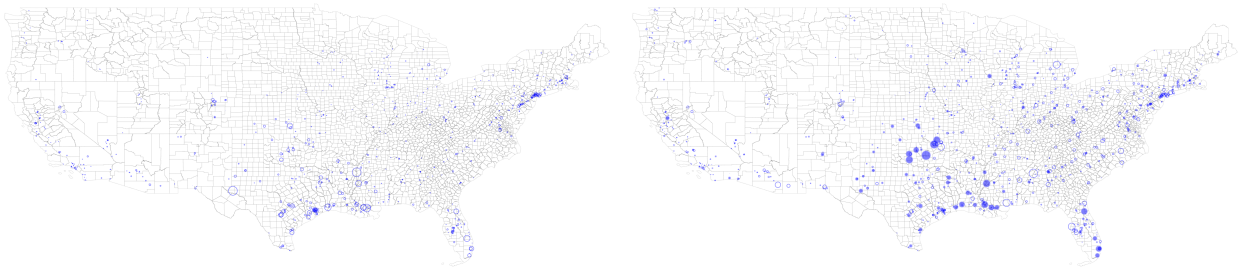
as here fracking provided a natural experiment with plausibly large enough variation in a

local amenity to meaningfully impact location utility.

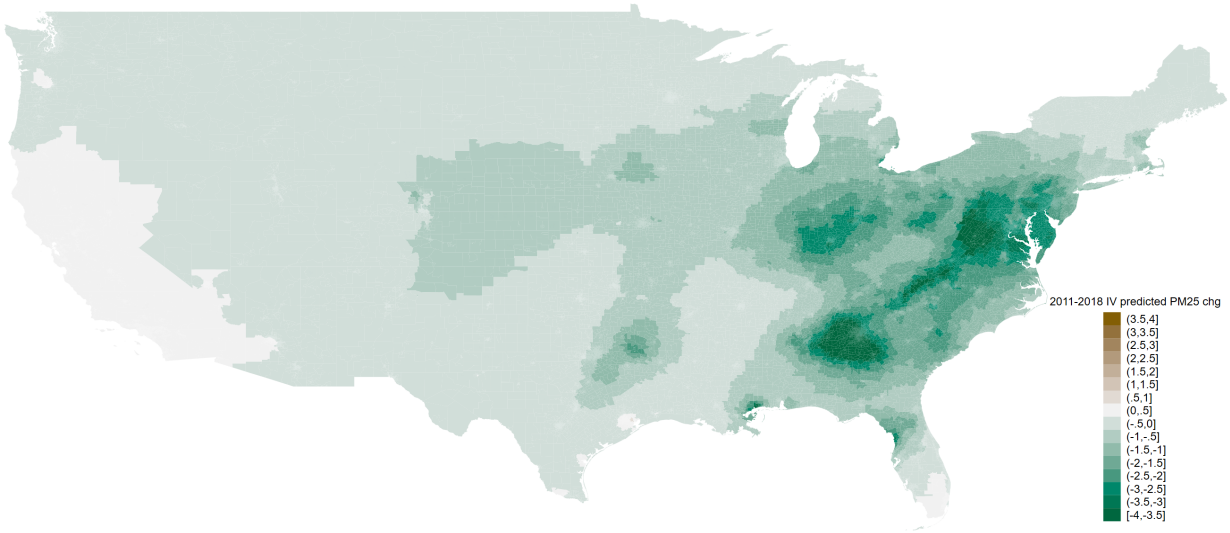
Figure 3: Effects of fracking on electricity emissions by fuel type and predicted $PM_{2.5}$



(a-b) Coal generators: predicted (a) and observed (b) NO_x change during 2011-2018



(c-d) Natural gas generators: predicted (c) and observed (d) NO_x change during 2011-2018



(e) Predicted $PM_{2.5}$ Changes, 2011–2018

NOTES: Panels (a) and (b) show the coal generators' predicted (panel a) and observed (panel b) NO_x change during 2011–2018. Panels (c) and (d) show the natural gas generators' predicted (panel c) and observed (panel d) NO_x change during 2011–2018. Solid circles represents decreases and hollow circles represents increases. Predicted pollution concentrations changes in the U.S. are based on the estimation procedure described in Section 4.2.

Let $\mathbf{W}^p$ be the p-pollutant source-receptor matrix (SRM), where element w^p_{gj} indicates the amount of secondary $PM_{2.5}$ pollution (in $\mu g/m^3$) received by census tract j from a one unit emission of primary pollutant p from EGU g. Total secondary $PM_{2.5}$ concentration (in $\mu g/m^3$) in location j and year t is then the product of a facility's p predicted emissions, $\widehat{E}^p_{gt}$, and its conversion to $PM_{2.5}$ concentrations in location i, summed over all facilities and pollutants. Denote that as $\widehat{X}_{jt} = \sum_p \sum_g w^p_{gj} \widehat{E}^p_{gt}$.

Next, recall the housing cost and amenity decomposition in equation (4) and (5), which are inserted into the expression for $\delta^{\ell r}_{jt}$ in equation (6). We instrument for x_{jt} and z_{jt} with the following two first stage regressions:

$$x_{jt} = \phi_{11}\widehat{X}_{jt} + \phi_{12}\widehat{Z}_{jt} + \varsigma_{1jt} \tag{11}$$

$$z_{jt} = \phi_{21}\widehat{X}_{jt} + \phi_{22}\widehat{Z}_{jt} + \varsigma_{1jt}, \tag{12}$$

where $\widehat{Z}_{jt} = \sum_{k \neq j} s_{jk}\widehat{X}_{kt}$ is the distance-weighted fracking-induced air quality in locations $k \neq j$. In doing so, the reduced-form $\beta^{\ell r}_0$ and $\beta^{\ell r}_1$ capture all the direct and indirect effects of air quality on unobserved utility locally, as well as spillover effects that exhibit a distance gradient.

To conclude our argument that our instruments are valid in this setting, we demonstrate their relevance for predicting air quality with the first stage results with tract and year fixed effects in Table A3 for our empirical setting of the Chicago CBSA. We can see that our instruments have predictive power on air quality, explaining almost a third of ambient air quality over 2011–2018. Figure A9 shows the cross-sectional variation in our instrument; it maps the air quality improvements implied by these predictions for each Chicago CBSA census tract. In terms of the exclusion restriction, we argue that the air pollution changes in census tract j explained by shale gas propensity modulated by pipeline density as of the year 2000 are unlikely to be correlated with other time-varying factors that impact utility which are also correlated with shale gas propensity and pipeline network. Note that the argument only needs to exclude time-varying factors, since our regression to estimate the combined impact parameters in equation (6) includes year and location fixed effects.

To allow utility to vary flexibly in own and remote air quality, we estimate the following non-parametric version of equation (6), where the left hand side is replaced with our estimates $\widehat{\delta_{jt}^{\ell r}}$ from the sorting model:

$$\widehat{\delta_{jt}^{\ell r}} = f(x_{jt}, z_{jt}; \mathcal{B}) + \gamma_j^{\ell} + \mu_t^{\ell} + e_{jt\ell}. \tag{13}$$

We evaluate the performance of alternative non-parametric models for equation (13), using natural restricted cubic splines of own and remote air quality. We vary the number of knots used in the cubic spline: $\{3, 4, 5\}$; the number of 10km distance bands included in the set z of neighboring census tracts: $\{2, 3, 4, 5, 6\}$, and function used to measure neighboring tracts distance: euclidean, exponential, inverse hyperbolic sine, and log. The AIC and BIC across models are shown in Table A4. We choose the model with the lowest AIC and BIC, which is a model with three knots, two neighbor distance bands, and an exponential function of distance.

Appendix D considers another plausible instrument in this setting: $PM_{2.5}$ attributable to only electricity generation from sources outside of the Chicago CBSA. This appendix discusses the merits of this alternative approach and presents the corresponding main results figure with this instrument in Figure A12, which are very similar to the forthcoming results in Figure 5.

5 Results

5.1 Parameter estimates

Estimates of moving costs from our sorting model are provided in Table 2. Our model is in utility and not dollars, so these estimates are interpreted as such. As shown in equation 2, our model includes demographic-by-income-specific costs or frictions to moving, which we operationalize by estimating a baseline moving cost estimate as well as race/ethnicity- and income- specific parameters that modulate the baseline moving cost up or down compared to the excluded group, which is white renters in the highest income quartile (4). Moving

Table 2: Sorting model parameter estimates

	Estimate	Std errors
ζ Moving cost, baseline	-11.39	(.0626)
$\zeta^{b\cdot 1}$ Moving cost, Black-w1 (lowest income)	1.39	(.0784)
$\zeta^{b\cdot 2}$ Moving cost, Black-w2	1.77	(.088)
$\zeta^{b\cdot 3}$ Moving cost, Black-w3	1.11	(.1418)
$\zeta^{b\cdot 3}$ Moving cost, Black-w4 (highest income)	2.62	(.1623)
$\zeta^{w\cdot 1}$: Moving cost, white-w1 (lowest income)	0.71	(.0968)
$\zeta^{w\cdot 2}$: Moving cost, white-w2	-1.15	(.138)
$\zeta^{w\cdot 3}$: Moving cost, white-w3	0.80	(.0756)
$\zeta^{w\cdot 4}$: Moving cost, white-w4 (highest income)	NA	(—)
$\zeta^{w\cdot 1}$: Moving cost, Hispanic-w1 (lowest income)	-0.05	(.1673)
$\zeta^{w\cdot 2}$: Moving cost, Hispanic-w2	1.18	(.1079)
$\zeta^{w\cdot 3}$: Moving cost, Hispanic-w3	-0.56	(.2128)
$\zeta^{w\cdot 4}$: Moving cost, Hispanic-w4 (highest income)	-0.11	(.3628)

NOTES: Asymptotic standard errors are computed from the inverse of the Hessian matrix, which is obtained numerically.

costs enter the utility function positively, so a negative value indicates frictions to moving. In our model, our moving cost estimates will capture any and all frictions involved with moving to a new census tract in the Chicago CBSA, from the monetary costs associated to the move, to the psychological costs of leaving your home, or finding new employment to any race/ethnicity based discrimination in household choice set of amenities available in different locations. Income type 1 corresponds to the lowest income group, and income type 4 corresponds to the highest. Our estimates find that Black renters have slightly lower moving costs in all income groups compared to the excluded group. White renters in the first and third income groups have lower moving costs as well, while white renters in the second lowest income group have higher moving costs. Hispanics in all income types have higher moving costs except in the second lowest income group.

5.2 Impacts of the policies on welfare and pollution gaps

We use the moving cost estimates together with our estimates of location-year-income-race/ethnicity specific components of location utility, $\widehat{\delta_{jt}^{\ell r}}$, to construct expected welfare in 2011 and counterfactual air pollution states. We estimate the welfare effects of four counterfactual simulations that improve local air quality in the Chicago CBSA, as well as from

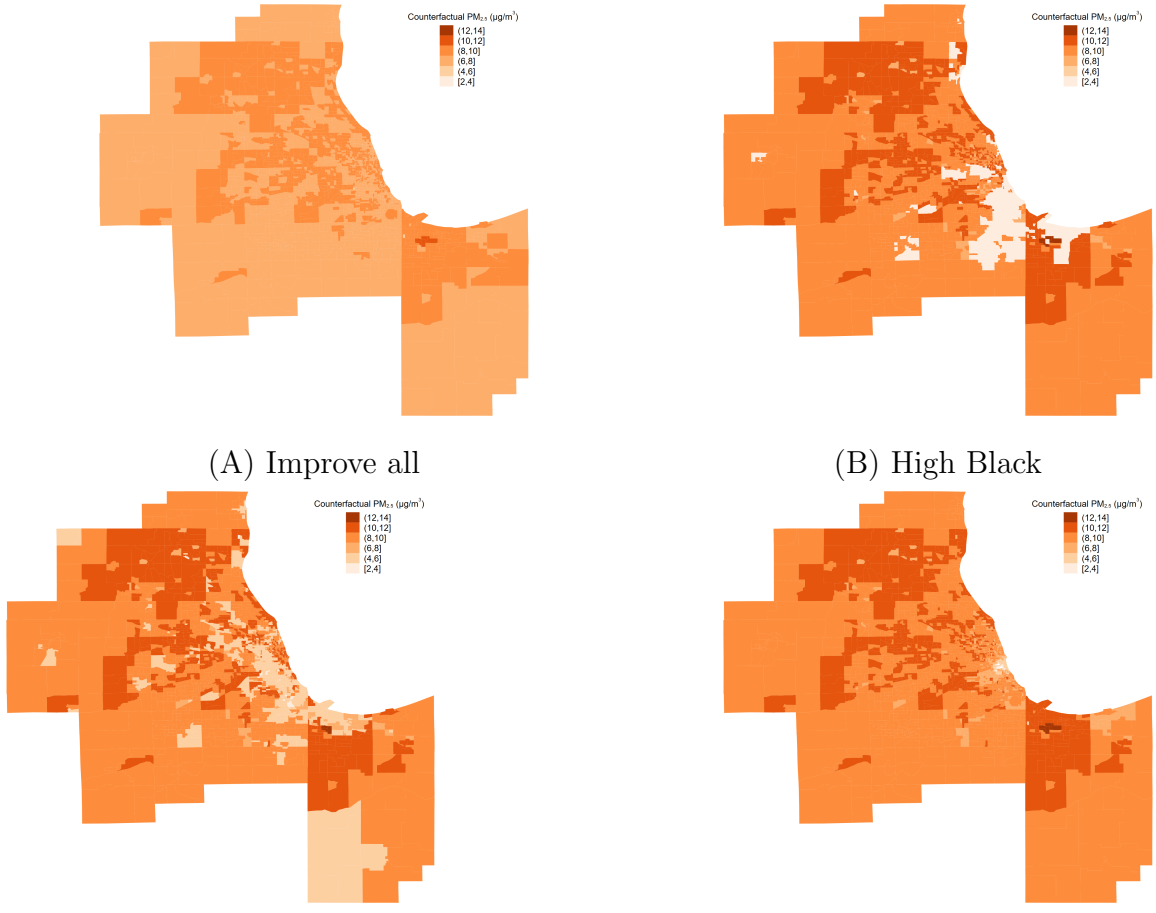
the observed air quality improvements in 2018. Each simulation of expected welfare in a counterfactual state starts with the unobserved location utilities and expected welfare estimated in 2011. Then, we model the effect of a change in air quality on $\widehat{\delta_{jt}^{\ell r}}$ using the estimated parameters from a non-parametric version of equation (6). With the new $\widehat{\delta_{jt}^{\ell r}}$, we estimate expected welfare in the counterfactual air pollution state. Then, for a given race/ethnicity, we calculate the change in welfare across the two states. We use the same approach to estimate the effects of the observed pollution improvements in 2018—that is, we estimate the impact of these improvements by simulating a new $\widehat{\delta_{jt}^{\ell r}}$ with observed 2018 pollution improvements, instead of using the $\widehat{\delta_{jt=2018}^{\ell r}}$ from the sorting model. The reason for this is that the latter estimate would include other changes to location utility in 2018 not related to air pollution changes. We use our estimates of type-specific changes in expected welfare to construct the difference in differences metric in equation (1). We construct this metric to compare outcomes for Black to white renters, as well to compare outcomes for Hispanic to white renters. In constructing this metric, an additional contraction mapping is performed to recover the expected share of each type's population that lives in each tract in the counterfactual simulations.

Our simulated policies have unique spatial patterns of pollution improvements. The first simulation improves local air quality for each tract in the Chicago CBSA by an equal percentage. The percentage is selected such that the aggregate air quality improvement in this simulation corresponds to the aggregate air quality improvement observed in the CBSA from 2011 to 2018. We call this the *Improve All* simulation. The second simulation achieves the same aggregate pollution reduction, but targets air quality improvements in tracts in the Chicago CBSA with the top tercile of Black residents, which we call the *High Black* simulation. The third simulation achieves the same aggregate pollution reduction, but targets air quality improvements in tracts identified as priority tracts to target improvement in the Biden-Harris administration's Climate and Economic Justice Screening Tool. Since these tracts have a high degree of correlation with poverty rate and income, we call this the *Low Income* simulation.[13] The fourth simulation shuts down two power plants in the

[13]Rudik, Lemoine and Marcheva (2025) find that 94% of tracts above the 65th percentile of the poverty rate qualify are categorized as disadvantaged in the EJ40 program.

Chicago CBSA, the Crawford and Fisk plants, located in the eastern region of the CBSA and operating on coal and diesel oil, respectively. The simulation reflects a practical policy approach—shutting down local pollution sources. The aggregate pollution from these two sources is below the aggregate reduction observed from 2011 to 2018, so this simulation's aggregate air quality improvement is not comparable to the other simulations. We call this the *Plant Shutdown* scenario. Figure 4 shows the air pollution concentration simulated in each scenario.

Figure 4: Air pollution in counterfactual simulations



(A) Improve all (B) High Black

(C) Low income (D) Plant shutdown

NOTES: This figure shows the air quality in concentrations of $PM_{2.5}$ across census tracts in the Chicago CBSA across the four counterfactual simulations.

Figure 5 plots the metrics in equation (1), (1″), and (1‴), denoted ΔW_ℓ, $\Delta\widetilde{x}_\ell$, and Δx_ℓ respectively. In this Figure, we took the mean of the results across the four income types, and result by income type provided in the Appendix Figure A2. The third row of panel (A)

and (B) presents our estimates of ΔW_ℓ, the change in the welfare gap moving from 2011 to the simulated air pollution state. The simulated air pollution states are delineated by color shading in legend. The third row of panel (A) shows that all simulated air pollution policies and the observed improvements generated reductions in the Black—white welfare gap. The third row of panel (B) shows that two of the simulated air pollution policies generated reductions in the Hispanic—white welfare gap.

The first two rows of each panel plot environmental outcomes. To measure these outcomes by demographic group d, for each simulation we estimate average per capita $PM_{2.5}$ for each simulated state by demographic group p^d, following the approach in Hernandez-Cortes, Meng and Weber (2023). That is, we construct p^d by multiplying the $PM_{2.5}$ concentration in a census tract by the number of renters of that group, taking the sum of those values over the Chicago CBSA, then dividing by the total population of that group. This measure describes the $PM_{2.5}$ in the location where the average person of demographic group d resides. We compute this metric in 2011 and then each simulated state, and construct the difference of differences that corresponds to $\Delta\widetilde{x}_\ell$ and Δx_ℓ. For these comparisons, the differencing across states is simulated state outcome less the outcome in 2011, so that a positive value indicates a pollution reduction (improvement in air quality) compared to 2011. The first row of each panel shows $\Delta\widetilde{x}_\ell$, which corresponds to a no-sorting framework. In other words, the row shows the change in pollution gap assuming that all the renters stay in the location they reside in 2011. The second row of each panel shows Δx_ℓ, which corresponds to pollution outcomes with re-sorting. For this row, we estimate p^d in 2011 with the same approach as in the no-sorting setup. But, p^d in the simulated state is now constructed using our estimates of counterfactual location shares in the simulated states. These shares are obtained with an additional contraction mapping performed with the estimated $\widehat{\delta_{jt}^{\ell r}}$.

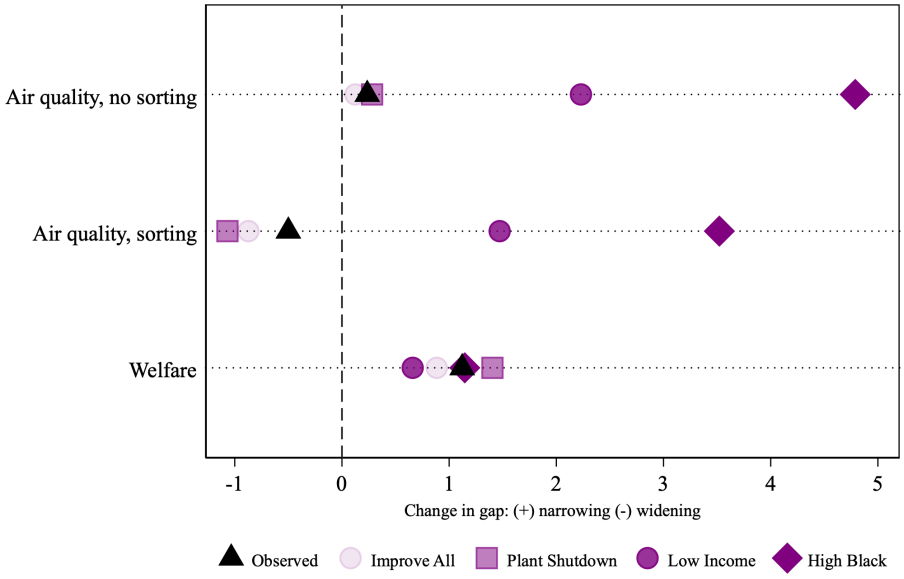
In both panels, simulated air quality states reduce pollution gaps when sorting is not accounted for. Both panels show that these reductions are attenuated or reversed when accounting for re-sorting. For the Black—white pollution gap, the effects of the *Improve All*, *Plant Shutdown*, and *Observed* on the pollution gap are reversed when accounting for re-sorting. That is, while the no-sorting framework predicts these policies would reduce Black—white pollution gaps, these effects are reversed after accounting for the fact that

renters may move following a reduction in pollution. The effects of the *Low Income* and *High Black* simulations are attenuated in the sorting compared to the no-sorting framework. In other words, these policies lead to reductions in pollution gaps in both frameworks, but the reductions are smaller after accounting for re-sorting after the pollution change. For the Hispanic—white pollution gap, the effects of the simulated policies are reversed in the *Plant Shutdown* policies, and attenuated in all other simulations. To summarize, the pollution gap is reduced in both frameworks under all simulated policies, except for the *Plant Shutdown* policy in the sorting framework, for which pollution gap outcomes are reversed.

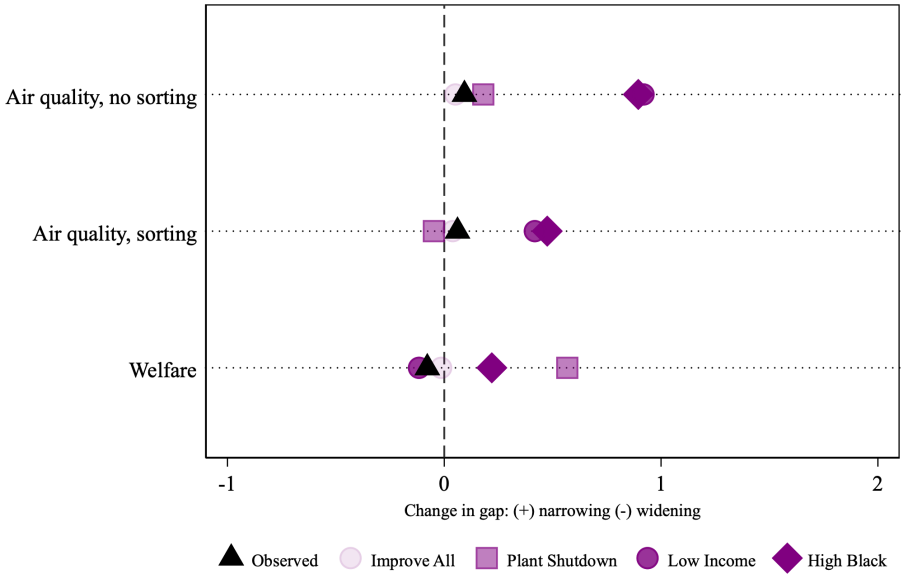
We now synthesize the collective results of the three metrics for both demographic group comparisons. First, we consider the differences in the predictions of environmental outcomes in a sorting versus no-sorting framework, where the latter assumes renters stay in their initial location following a pollution improvement. Overall, we find that accounting for sorting attenuates or reverses the gap reduction compared to a no-sorting framework. Next, we consider the results in rows two and three of both panels, the pollution gap with sorting and welfare gap metrics. For both demographic group comparisons, we find that reductions in welfare gaps can occur simultaneously with increases in the pollution gap. This is an important takeaway from our results with applied policy relevance: a demographically targeted pollution policy may look ineffective based on the environmental gap alone, while yielding improvements in the welfare gap. Next, we consider the results in rows one and two of each panel, the impacts on pollution gaps with and without accounting for sorting. Broadly, our results indicate that the effects of these policies on pollution gaps are attenuated, and in some cases reversed, when accounting for re-sorting following the pollution improvement compared to assuming renters stay in their initial locations. Finally, we discuss difference across the policies in terms of their impact on welfare. In panel (A) we find that all polices have a similar impact of welfare, regardless of their targetting approach. This is surprising given these approaches span from improving all locations by an equal percentage to targetting tracts with high share of Black residents. We take this as evidence that sorting nullifies some of the policies distributional intents, though all the policies do reduce Black—white welfare gaps.

Figure 5: Change in welfare and pollution gaps

(A) Black—white



(B) Hispanic—white



NOTES: The rows of each sub figure show the estimates of $\Delta\widetilde{x}$, Δx, and ΔW, equation $(1^{'})$, $(1^{''})$, and (1) respectively. Panel (A) shows shows the metric comparing Black to white renters, and panel (B) shows the metric comparing Hispanic to white renters.

6 Conclusion

This paper develops an approach for studying the impact of EJ-oriented and demographically targeted place-based policy on both environmental and welfare inequities. To do so, we develop a new approach for accounting for endogenous amenities in the context of residential location choice models. Provided the researcher has a source of exogenous variation in the amenity of interest, this method is applicable to a broad range of research questions on the impact of amenity changes on welfare. Our approach is straightforward to implement and does not require observations of indirectly affected amenities nor functional form assumptions around indirect effects.

Much of the environmental justice literature to date has focused on changes in pollution gaps (Cain et al., 2024). We complement this work by evaluating policies in terms of both pollution and welfare gaps. We formally describe each of these related metrics, and quantify the impacts of alternative policy simulations on each. Our welfare metric emerges from our discrete choice location model, and we demonstrate that when the research question regards relative changes across demographic groups within an income group, the question can be answered without recovering the marginal utility of income, which is generally very difficult to estimate in an unbiased way. Further, we demonstrate how to construct race/ethnicity-by-income-specific location-utility and expected welfare measures that do require estimating race/ethnicity-specific preferences for amenities. We take this approach given the difficulty of separating out race/ethnicity-specific preferences from discriminatory factors. Thus, our results can be interpreted as the effects of policies inclusive of any discriminatory factors limiting access or enjoyment of certain amenities or locations.

Our empirical findings have three main takeaways. First, an EJ-oriented policy can look ineffective at narrowing racial pollution gaps, while at the same time narrowing welfare gaps. This is a cautionary tale for EJ policy evaluation—while the policy may not meet its stated environmental related goal, it can lead to reductions in welfare gaps. Second, we find that while a policy can appear to reduce racial pollution gaps when sorting is ignored, including re-sorting following the pollution change can attenuate or reverse those effects. Third, we find minimal differences in policies' welfare impacts even while targetting approaches diverge,

suggest that re-sorting nullifies some of the policies' initial intent.

It is important to caveat that our results describe the outcomes for renters and are not applicable to home owners. The incentives for renters are different from those of owners, as owners have the ability to capitalize local amenity improvements in future home sales. Owners have a unique location choice model with new forms of moving frictions and likely forward looking expectations (Bayer et al., 2016). Studying the pollution and welfare effects of these policies on homeowners is a fruitful topic for future work. It is also important to note that our paper does not provide any insight on the extent to which race/ethnicity-based discriminatory factors are mediating our results. The advantage of our approach is that we do not have to pursue the difficult task of separating race or ethnicity-correlated preferences from discrimination. The drawback of our approach is that we do not separately identify the role of discrimination in shaping our findings. This is also an excellent topic for future work.

References

Bakkensen, Laura A, and Lala Ma. 2020. "Sorting over flood risk and implications for policy reform." *Journal of Environmental Economics and Management*, 104: 102362.

Banzhaf, Spencer, Lala Ma, and Christopher Timmins. 2019. "Environmental Justice: The Economics of Race, Place, and Pollution." *Journal of Economic Perspectives*, 33(1): 185–208.

Bartik, Alexander W, Janet Currie, Michael Greenstone, and Christopher R Knittel. 2019. "The local economic and welfare consequences of hydraulic fracturing." *American Economic Journal: Applied Economics*, 11(4): 105–55.

Bayer, Patrick, Fernando Ferreira, and Robert McMillan. 2007. "A unified framework for measuring preferences for schools and neighborhoods." *Journal of political economy*, 115(4): 588–638.

Bayer, Patrick, Robert McMillan, Alvin Murphy, and Christopher Timmins. 2016. "A dynamic model of demand for houses and neighborhoods." *Econometrica*, 84(3): 893–942.

Berry, Steven, James Levinsohn, and Ariel Pakes. 1995. "Your use of the JSTOR archive indicates your acceptance of the Terms & Conditions of Use, available at http://about. jstor. org/terms." *Econometrica*, 63(4): 841–890.

Bondy, Malvina, Sefi Roth, and Lutz Sager. 2020. "Crime is in the air: The contemporaneous relationship between air pollution and crime." *Journal of the Association of Environmental and Resource Economists*, 7(3): 555–585.

Bowen, William. 2002. "An Analytical Review of Environmental Justice Research: What do we Really Know?" *Environmental Management*, 29(1): 3–15.

Bullard, Robert. 2000. *Dumping in Dixie: Race, Class, and Environmental Quality.* Westview Press.

Cain, Lucas, Danae Hernandez-Cortes, Chris Timmins, and Paige Weber. 2024. "Recent Findings and Methodologies in Economics Research in Environmental Justice." *Review of Environmental Economics and Policy*.

Christensen, Peter, and Christopher Timmins. 2022. "Sorting or steering: The effects of housing discrimination on neighborhood choice." *Journal of Political Economy*, 130(8): 2110–2163.

Christensen, Peter, Ignacio Sarmiento-Barbieri, and Christopher Timmins. 2022. "Housing discrimination and the toxics exposure gap in the United States: Evidence from the rental market." *Review of Economics and Statistics*, 104(4): 807–818.

Colmer, Jonathan, Ralf Martin, Mirabelle Muûls, Ulrich J Wagner, et al. 2020. "Does pricing carbon mitigate climate change? Firm-level evidence from the European Union emissions trading scheme." *Center for Economic Performance Discussion Paper*, , (1728).

Currie, Janet, Eric A Hanushek, E Megan Kahn, Matthew Neidell, and Steven G Rivkin. 2009. "Does pollution increase school absences?" *The Review of Economics and Statistics*, 91(4): 682–694.

Currie, Janet, John Voorheis, and Reed Walker. 2020. "What Caused Racial Disparities in Particulate Exposure to Fall? New Evidence from the Clean Air Act and Satellite-Based Measures of Air Quality." National Bureau of Economic Research Working Paper 26659.

Depro, Brooks, Christopher Timmins, and Maggie O'Neil. 2015. "White Flight and Coming to the Nuisance: Can Residential Mobility Explain Environmental Injustice?" *Journal of the Association of Environmental and Resource Economists*, 2(3): 439–468.

Diamond, Rebecca. 2017. "Housing supply elasticity and rent extraction by state and local governments." *American Economic Journal: Economic Policy*, 9(1): 74–111.

Goodkind, Andrew L, Christopher W Tessum, JS Coggings, Jason D Hill, and Julian D Marshall. 2019. "InMAP source-receptor matrix (ISRM) dataset."

Hausman, Catherine, and Ryan Kellogg. 2015. "Welfare and distributional implications of shale gas." National Bureau of Economic Research.

Hausman, Catherine, and Samuel Stolper. 2021. "Inequality, information failures, and air pollution." *Journal of Environmental Economics and Management*, 110: 102552.

Heblich, Stephan, Alex Trew, and Yanos Zylberberg. 2021. "East-side story: Historical pollution and persistent neighborhood sorting." *Journal of Political Economy*, 129(5): 1508–1552.

Hernandez-Cortes, Danae, Kyle C Meng, and Paige Weber. 2023. "Decomposing Trends in US Air Pollution Disparities from Electricity." *Environmental and Energy Policy and the Economy*, 4(1): 91–124.

Herrnstadt, Evan, and Erich Muehlegger. 2015. "Air pollution and criminal activity: Evidence from Chicago microdata." National Bureau of economic research.

Jacobsen, Grant D. 2019. "Who wins in an energy boom? Evidence from wage rates and housing." *Economic Inquiry*, 57(1): 9–32.

Liang, Yuanning, Ivan Rudik, Eric Yongchen Zou, Alison Johnston, Amanda D Rodewald, and Catherine L Kling. 2020. "Conservation cobenefits from air pollution regulation: Evidence from birds." *Proceedings of the National Academy of Sciences*, 117(49): 30900–30906.

Liu, Haoming, and Alberto Salvo. 2018. "Severe air pollution and child absences when schools and parents respond." *Journal of Environmental Economics and Management*, 92: 300–330.

Liu, Zhaoyang, Nick Hanley, and Danny Campbell. 2020. "Linking urban air pollution with residents' willingness to pay for greenspace: A choice experiment study in Beijing." *Journal of Environmental Economics and Management*, 104: 102383.

Mohai, Paul, David Pellow, and J. Timmons Roberts. 2009*a*. "Environmental Justice." *Annual Review of Environment and Resources*, 34(1): 405–430.

Mohai, Paul, David Pellow, and J Timmons Roberts. 2009*b*. "Environmental justice." *Annual review of environment and resources*, 34: 405–430.

Persico, Claudia, David Figlio, and Jeffrey Roth. 2020. "The developmental consequences of superfund sites." *Journal of Labor Economics*, 38(4): 1055–1097.

Ringquist, Evan J. 2005. "Assessing Evidence of Environmental Inequities: A Meta-analysis." *Journal of Policy Analysis and Management*, 24(2): 223–247.

Rosen, Sherwin. 1974. "Hedonic prices and implicit markets: product differentiation in pure competition." *Journal of political economy*, 82(1): 34–55.

Rudik, Ivan, Derek Lemoine, and Antonia Marcheva. 2025. "Equity and efficiency in the Bipartisan Infrastructure Law's adaptation investments." *Environmental and Energy Policy and the Economy*, 6(1): 65–100.

Tessum, Christopher W, David A Paolella, Sarah E Chambliss, Joshua S Apte, Jason D Hill, and Julian D Marshall. 2021. "PM2. 5 polluters disproportionately and systemically affect people of color in the United States." *Science advances*, 7(18): eabf4491.

Tessum, Christopher W., Jason D. Hill, and Julian D. Marshall. 2017. "InMAP: A model for air pollution interventions." *PLOS ONE*, 12(4): 1–26.

Tessum, Christopher W., Joshua S. Apte, Andrew L. Goodkind, Nicholas Z. Muller, Kimberley A. Mullins, David A. Paolella, Stephen Polasky, Nathaniel P. Springer, Sumil K. Thakrar, Julian D. Marshall, and Jason D. Hill. 2019. "Inequity in consumption of goods and services adds to racial–ethnic disparities in air pollution exposure." *Proceedings of the National Academy of Sciences*, 116(13): 6001–6006.

Train, Kenneth E. 2009. *Discrete choice methods with simulation.* Cambridge university press.

U.S. EIA, The U.S. Energy Information Administration. 2017. "Competition between coal and natural gas affects power markets."

U.S. EIA, U.S. Energy Information Administration. 2018. "Hydraulically fractured horizontal wells account for most new oil and natural gas wells."

Van Donkelaar, Aaron, Melanie S Hammer, Liam Bindle, Michael Brauer, Jeffery R Brook, Michael J Garay, N Christina Hsu, Olga V Kalashnikova, Ralph A Kahn, Colin Lee, et al. 2021. "Monthly global estimates of fine particulate matter and their uncertainty." *Environmental Science & Technology*, 55(22): 15287–15300.

Wang, Wen. 2021. "Environmental Gentrification."

Wang, Xiao, George Deltas, Madhu Khanna, and Xiang Bi. 2021. "Community Pressure and the Spatial Redistribution of Pollution: The Relocation of Toxic-Releasing Facilities." *Journal of the Association of Environmental and Resource Economists*, 8(3): 577–616.

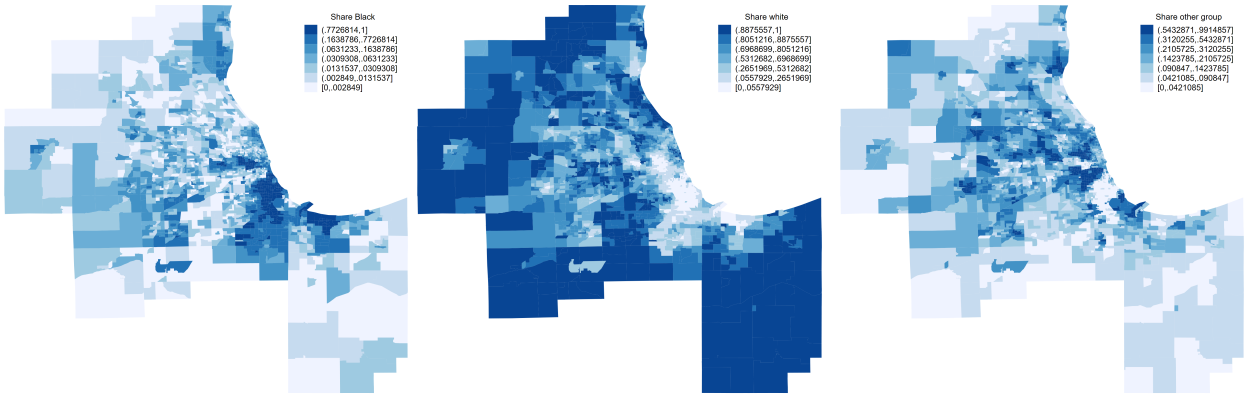
A Appendix: additional descriptives and results

Table A1: Mobility among renters and owners, average 2011–2018 (ACS 5)

	(1)	(2)
	All census tracts	Chicago census tracts
Renters (%)	0.355	0.360
	(0.23)	(0.23)
Owners (%)	0.645	0.640
	(0.23)	(0.23)
Owners - moved from last year (%)	0.073	0.064
	(0.06)	(0.05)
Renters - moved from last year (%)	0.265	0.246
	(0.14)	(0.14)
Owners - moved within same county (%)	0.043	0.044
	(0.04)	(0.04)
Renters - moved within same county (%)	0.161	0.165
	(0.11)	(0.11)
Owners - moved diff. county within same state (%)	0.015	0.010
	(0.02)	(0.02)
Renters - moved diff. county within same state (%)	0.053	0.037
	(0.07)	(0.07)
Owners - moved diff. state (%)	0.011	0.008
	(0.02)	(0.02)
Renters - moved diff. state (%)	0.041	0.033
	(0.06)	(0.05)
Owners - moved from abroad (%)	0.004	0.003
	(0.02)	(0.01)
Renters - moved from abroad (%)	0.009	0.011
	(0.03)	(0.03)
pct_movers_abroad	0.003	0.003
	(0.02)	(0.01)
pct_renters_abroad	0.009	0.011
	(0.03)	(0.03)
Observations	502296	15415

NOTES: Average mobility among renters and owners in census tracts at the national level (column 1) and in the Chicago CBSA during 2011–2018.

Figure A1: Population shares by race

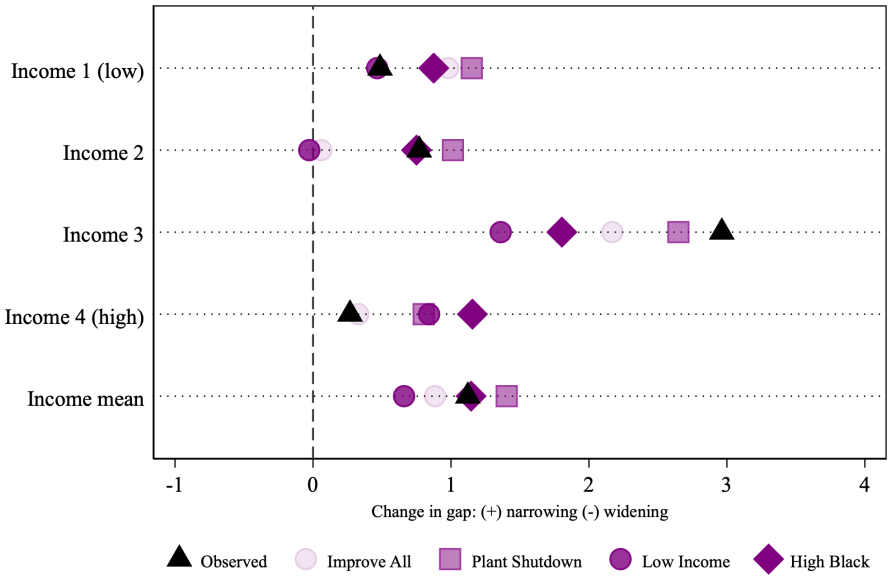


Share Black Share white Share other

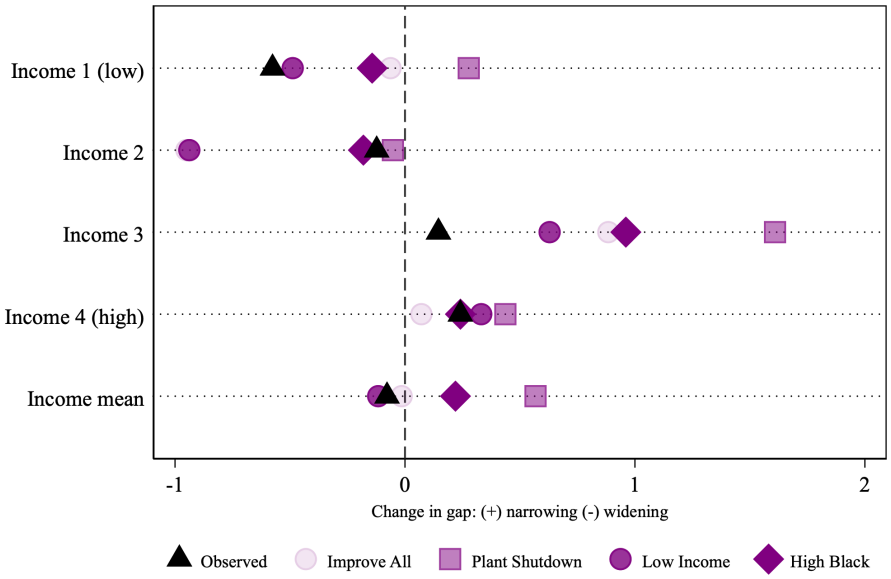
NOTES: Figures show share of different demographic groups in Chicago CBSA.

Figure A2: Change in gap by income type

(A) Black—white

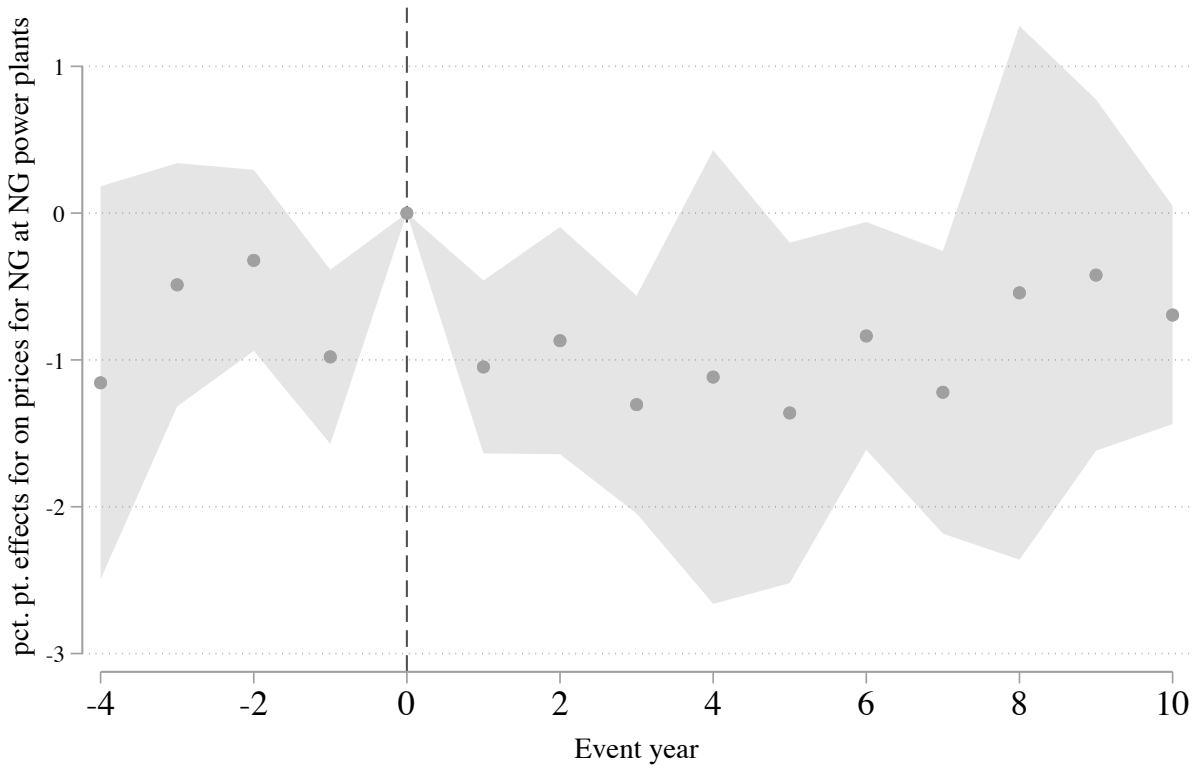


(B) Hispanic—white



NOTES: Each sub panel shows the estimates ΔW from equation (1), by income type. Panel (A) shows shows the metric comparing Black to white renters, and panel (B) shows the metric comparing Hispanic to white renters.

Figure A3: Event study with fracking-predicted emissions and EIA-923 natural gas prices as dependent variable



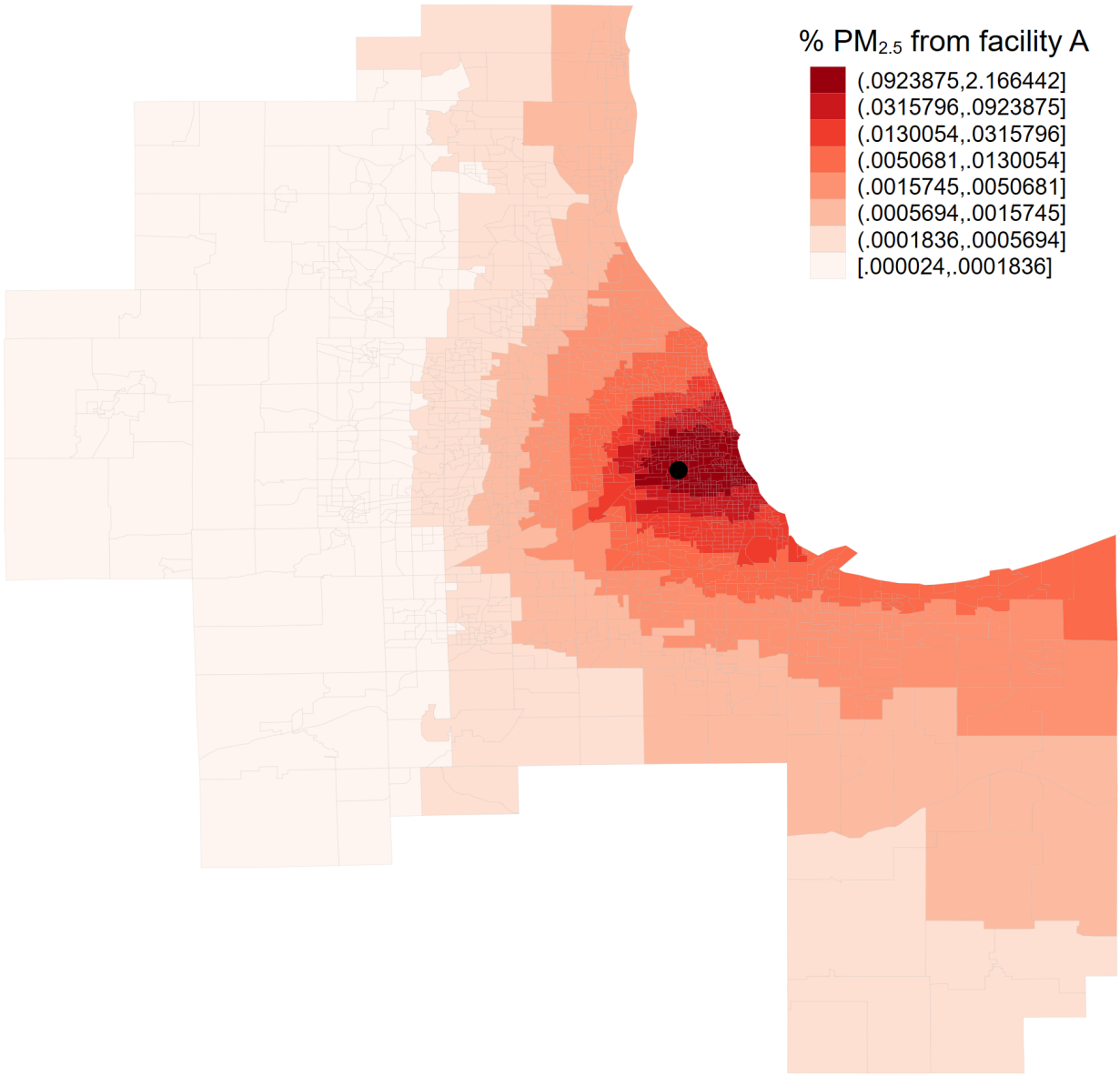
NOTES: This figure shows the results from the event study presented in Section 4.2 with plant-level natural gas prices as the dependent variable. Plant-level natural gas prices are obtained from EIA-923 data, which reports plant-level fuel receipts and costs. Since the dependent variable is at the plant and not unit-level, the event study regression here includes plant (not unit) fixed effects. Event year and data year fixed effects are also included.

B Appendix: Air quality data

Estimating our model requires time-varying changes in tract-level ambient air quality that are explained by our instrument. This section of the appendix provides further evidence that there is variation in ambient air quality in our study region during our sample period. Appendix C provides additional results related to the instrument used for air quality. We discuss the variation in our air quality data over time and space and corroborate those findings with other data sources.

Our instrument leverage variation in air quality due to variation in the location of pollution sources and pollution transport. Electric generating units emit $PM_{2.5}$ precursor pollutants from tall smokestacks. This allows pollution to travel on the basis of physical and chemical processes. These transport patterns create variation in which census tracts receive pollution from the same polluting source. We use InMAP to model these pollution transport patterns. Figure A4 provides an example of the cross-sectional variation provided by the transport patterns from pollutants from a coal-fired electric generating unit located in the Chicago CBSA based on InMAP. In this figure, we modeled a uniform increase of 1000 kg of $PM_{2.5}$ precursors using InMAP. This figure demonstrates that reducing the pollution from one plant would have unique effects on the air quality of different local census tracts. Likewise, reducing emissions from the set of coal units that generate emissions that create pollution for Chicago tracts will create unique patterns of improvement across census tracts.

Figure A4: Pollution concentrations from observed emissions of two facilities in Chicago CBSA

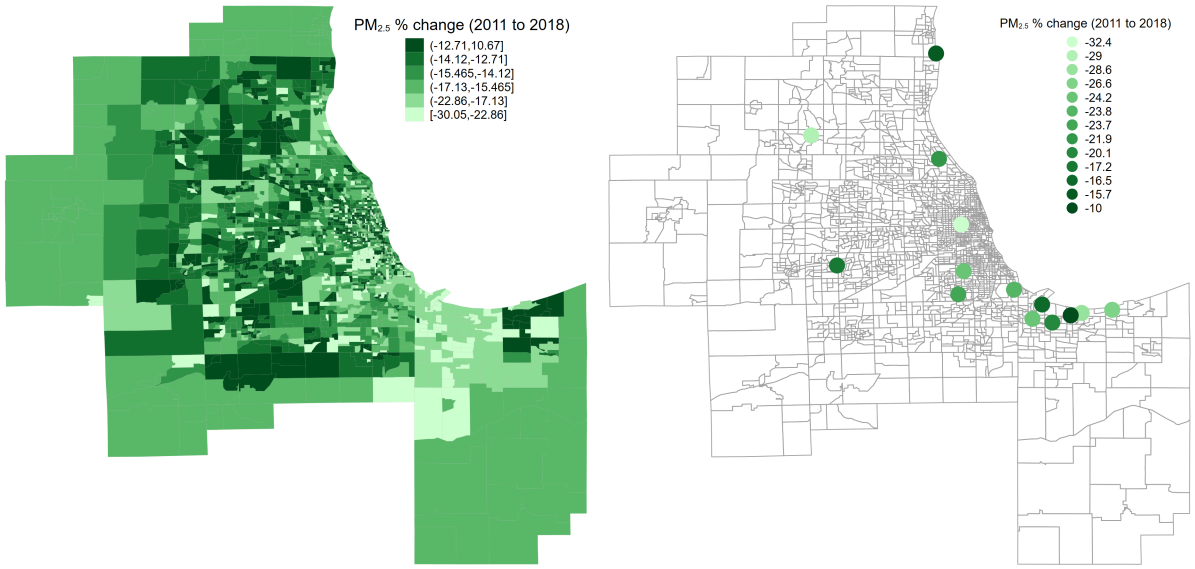


NOTES: Figures show pollution concentrations associated to a coal power plants (ORISPL code: 867) in the Chicago CBSA.

Figure A5 shows the variation in ambient air quality over the study period in the Chicago CBSA using the data from Van Donkelaar et al. (2021), which provides annual $PM_{2.5}$ at a 1km $\times$ 1km resolution. The figure shows that while concentrations of $PM_{2.5}$ reduced for all tracts in the Chicago CBSA over the period 2011–2018, the range of improvement varied from 10–30% reduction in $PM_{2.5}$ in 2018 compared to 2011.

The Van Donkelaar et al. (2021) is a re-analysis data product and as such might include measurement errors. We use hourly $PM_{2.5}$ readings from EPA air quality monitors to study air quality trends during the same period. The monitors have the advantage of providing

Figure A5: Changes in $PM_{2.5}$ 2011–2018

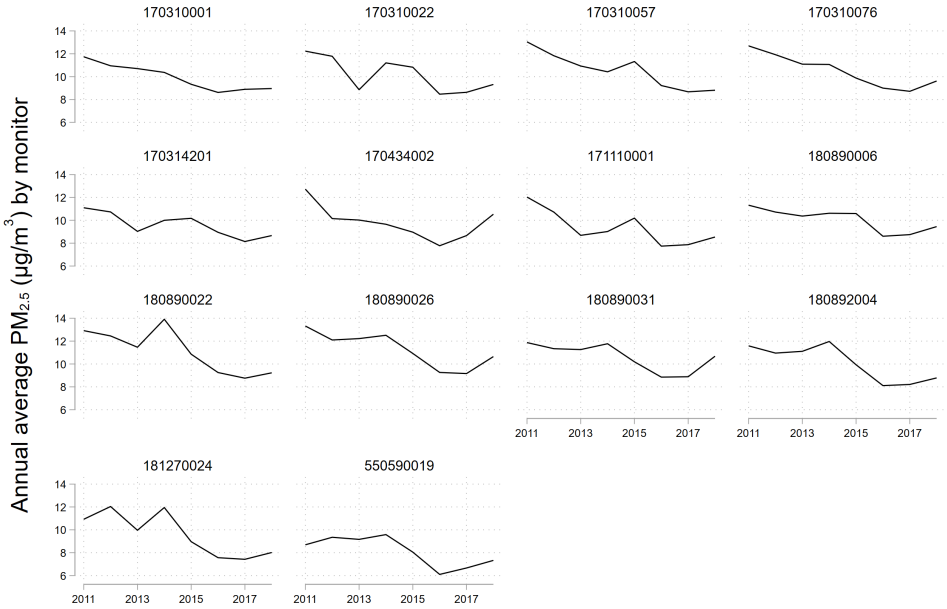


NOTES: Figures show changes in pollution concentrations from the Van Donkelaar et al. (2021) (left) and from EPA monitors (right).

hourly raw data, and thus potentially less measurement error than re-analysis products, but monitors only provide air pollution readings for distinct points in space, with insufficient geographic coverage for our research question. However, they are useful for comparing time series variation at the monitor locations. Figure A6 plots $PM_{2.5}$ concentrations at the 14 monitors available in the Chicago CBSA during our study period. The average change in the average annual monitor readings for 2018 compared to 2011 was 22 4%. The smallest reduction recorded by a monitor was 10%, while the largest was 32.5%. The results corroborate the time series variation found in the air quality data from Van Donkelaar et al. (2021), which we use in our main analysis.

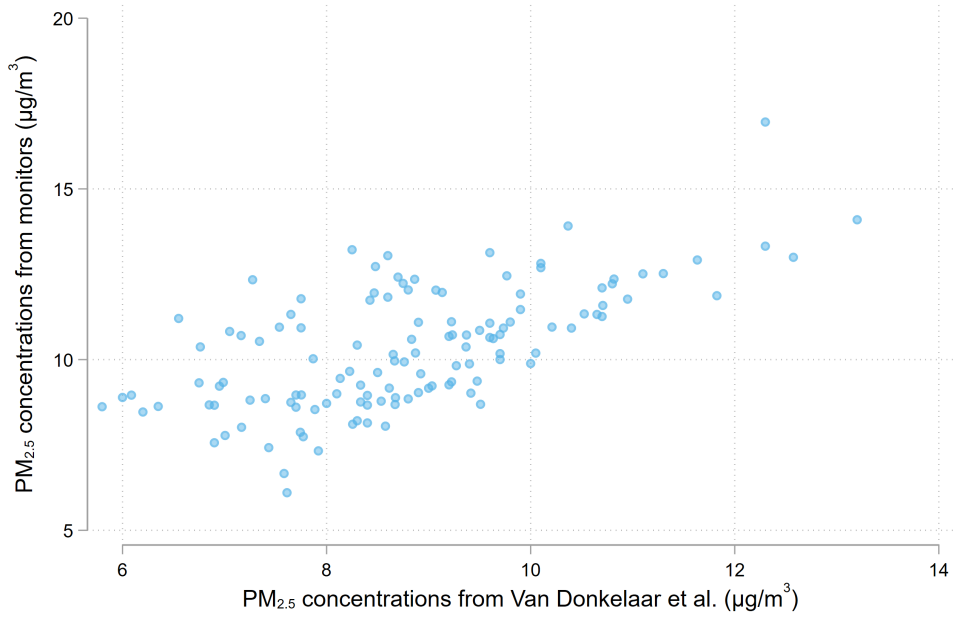
Figure A7 shows the correlation between pollution concentrations from EPA air quality monitors (assigned to the census tract where the monitor is located) and pollution concentrations from Van Donkelaar et al. (2021).

Figure A6: Pollution concentrations trends in Chicago CBSA EPA ambient air quality monitors



NOTES: This figure shows pollution concentrations from 14 pollution monitors in the Chicago CBSA. Each figure represents one pollution monitor's average annual readings from 2010–2018.

Figure A7: Correlation between pollution 2011-2018 concentrations from monitors and Van Donkelaar et al. (2021)



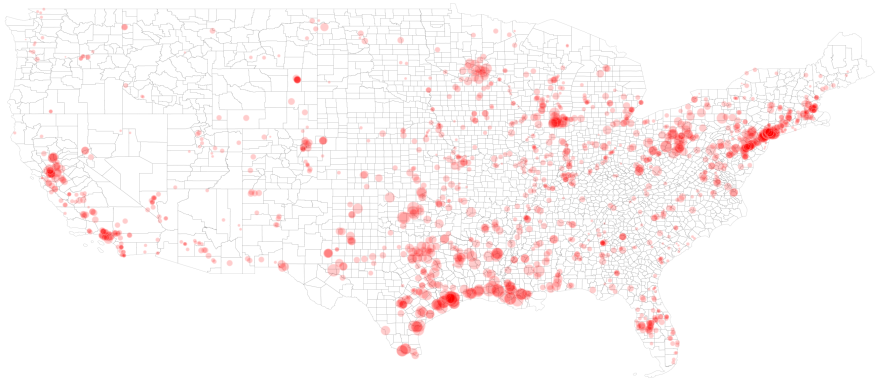
NOTES: This figure shows correlation between pollution concentrations from EPA ambient air quality monitors and satellite data from Van Donkelaar et al. (2021) during 2011-2018.

C Appendix: Air quality instrument

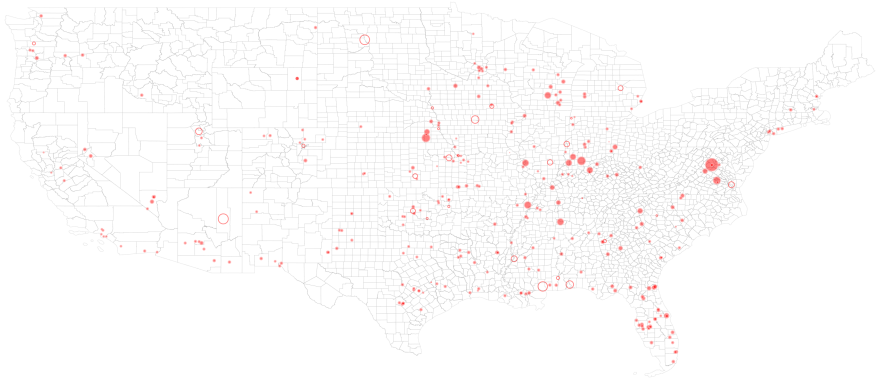
In our main results, we use fracking predicted $PM_{2.5}$ as an instrument for ambient $PM_{2.5}$ in a nonparametric estimation of equation (6). The construction of the instrumental variable is detailed in Section 4.2. Figure A8 shows the geographic variation in S_g, which we use as an instrument for EGU emissions.

Figure A8: Maps supporting the construction of instrument for air quality changes

(a) Generator-level potential natural gas supply from fracking (S_g)



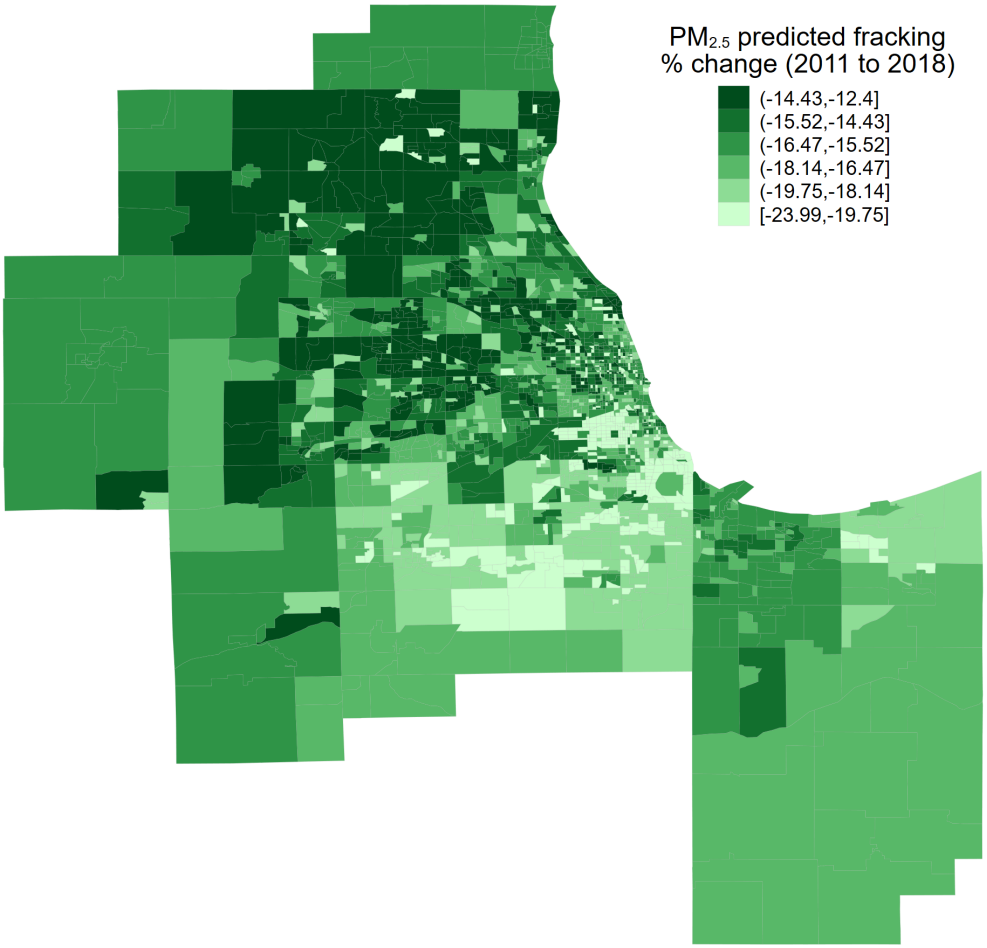
(b) Generator-level changes in observed natural gas prices



NOTES: Panel (a) shows potential fracking supply, defined in the text as the product of prospective fracking score and pipeline density. Panel (b) shows generator-level changes in observed natural gas input prices from EIA Form-923, where solid represents decreases in price change and hollow represents increases in price change.

Table A2 shows the results from the trend-break model estimates from equation (11). Figure A9 shows the changes in air quality predicted by our instrument in the Chicago CBSA. Table A3 reports the estimates from the first stage.

Figure A9: Predicted $PM_{2.5}$ in Chicago CBSA



NOTES: Predicted pollution concentrations changes in the U.S. and Chicago CBSA based on estimation procedure described in Section 4.2.

Table A2: Electricity emissions effects of fracking

	Outcome is (asinh) emissions and concentrations								
	(1)	(2)	(3)	(4)	(5)	(6)	(7)	(8)	(9)
		NO_x			SO_2			$PM_{2.5}$	
post×S_g×ng	13.937		-8.042	18.058		-0.208	13.331		-6.243
	(4.706)		(3.055)	(7.124)		(9.496)	(3.708)		(2.337)
post×S_g×coal	-35.022		-3.891	-34.933		-2.008	-27.385		-2.841
	(9.539)		(5.985)	(10.599)		(9.048)	(7.880)		(4.842)
trend×S_g×ng		-0.762	0.740		1.049	1.089		-0.097	1.069
		(1.191)	(0.927)		(1.747)	(0.666)		(0.823)	(0.730)
post×trend×S_g		4.084	3.092		1.963	1.935		2.961	2.191
×ng		(1.817)	(1.608)		(1.876)	(1.017)		(1.266)	(1.142)
trend×S_g×coal		-1.889	-1.150		-0.071	0.299		-0.641	-0.100
		(1.513)	(1.044)		(1.771)	(0.769)		(1.132)	(0.760)
post×trend×S_g		-4.036	-4.545		-6.619	-6.857		-4.336	-4.710
×coal		(2.261)	(1.967)		(2.225)	(1.669)		(1.784)	(1.558)
Generators	4,922	4,922	4,922	4,922	4,922	4,922	4,922	4,922	4,922
Plants	1,182	1,182	1,182	1,182	1,182	1,182	1,182	1,182	1,182
Counties	691	691	691	691	691	691	691	691	691
Observations	68,604	68,604	68,604	68,604	68,604	68,604	68,604	68,604	68,604

NOTES: This table shows the trend-break model estimates from equation (11). Standard errors in parenthesis, p-values in brackets.

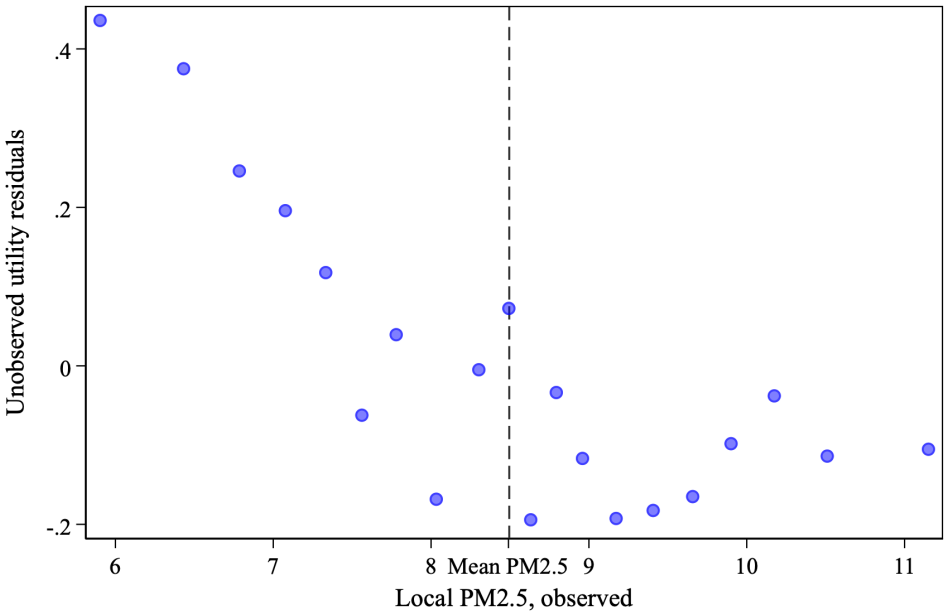
Our objective in estimating equation (6) is to allow location utility to vary flexibly in air quality, which is motivated by Figure A10. This figure plots the de-trended tract-year-income type estimated utility, $\widehat{\delta^{\ell}_{jt}}$, by the observed $PM_{2.5}$ for that tract-year. The de-trending is done by regressing the estimated $\widehat{\delta^{\ell}_{jt}}$ on income, tract, and year fixed effects. We obtain the residuals from that regression and plot them in a binned scatter plot below. Figure A10 shows a nonlinear relationship between the detrended utility and air quality; a linear fitted trend line would have a negative slope, with a lower detrended utility on average among tracts with higher air pollution.

Table A3: First stage of IV: Ambient $PM_{2.5}$ on Fracking-Predicted $PM_{2.5}$, Chicago CBSA 2011–2018

	Ambient $PM_{2.5}$
Predicted PM2.5	0.298***
	(0.000)
Tract FE	Yes
Year FE	Yes
Observations	22100
R-squared	0.958

NOTES: This table shows the results of a regression of tract-year ambient air quality measured in concentration of $PM_{2.5}$ (micrograms per meter cubed). Standard errors in parenthesis. $* \ p < 0.05$, $** \ p < 0.01$, $*** \ p < 0.001$.

Figure A10: Binned scatterplot of unobserved utility residuals on ambient air quality



NOTES: The y-axis are the residuals of a regression of location-year-income type utility estimates from the sorting model on fixed effects for location, year, and income type. These residuals are plotted by location-year air pollution levels on the x-axis. The vertical line shows the average $PM_{2.5}$ in Chicago CBSA over 2011–2018 for reference.

Table A4 presents the Akaike information criterion (AIC) and Bayes information criterion (BIC) for alternative nonparametric functions of equation (6). For this exercise we pool the estimates across income types and include a fixed effect for income type in all regressions. The models each use a natural restricted cubic spline, but vary in the number of knots used in the cubic spline: $\{3, 4, 5\}$; the number of 10km distance bands included in the set z of neighboring census tracts: $\{2, 3, 4, 5, 6\}$, and the function used to measure neighboring tract distance: Euclidean, exponential, inverse hyperbolic sine, log. As evident in Section 2, we do not directly interpret any of the coefficient estimates of the model to answer our

research questions. Rather we use the coefficients to predict unobserved tract-year-income type utility in simulations of counterfactual air quality states. Given these goals, we choose the nonparametric model with the lowest AIC and BIC. Table A4 shows that the model with exponential function of distance, two 10km distance bands of neighbors, and three knots in the cubic spline has the lowest AIC and BIC.

In our sorting model, the term δ_{jt}^{ℓ} includes many factors important to the residential location choice such as housing costs, school quality, and local crime. Here we show our instrument's explanatory power on some of these variables. Table A5 shows the results from several models that regress alternative location amenities on ambient air quality instrumented by fracking predicted air quality. The first column includes log rent prices as the dependent variable, which are obtained from proprietary data provider, Altos. In these data, each rental property-year is an observation in the data set. We observe the zip code of the property but not the census tract, so we match each rental property to the average annual zip code $PM_{2.5}$. To do so, we construct an area-weighted crosswalk of zip codes to census tract polygons, and use that to crosswalk our tract level $PM_{2.5}$, ambient and instrument, to the zip code level.

The tract-level dependent variables in subsequent columns are: (2) police arrests per population; (3) school attendance per population; (4) education spend per student; and (5) graduation rate per enrollment. The arrest data comes from the US FBI's Uniform Crime Reporting program. The data are at the zip code level, and for this analysis, we assume that arrest counts within each zip code are uniformly distributed across the census tract. To calculate an arrest rate per population, the arrest counts at the tract level were divided by the corresponding annual census tract population. School finance data at the school district level is obtained from the Annual Survey of School System Finances conducted by the U.S. Census. These data are available at the district level. We assign each tract the spending of the district in which it is contained. High school-level attendance and graduation rates from annual school report cards are published by the Department of Education for three states within the Chicago CBSA. Illinois, Indiana, and Wisconsin. Data is available at the zip code level, and we assign each tract the attendance and graduation rate for the zip code it is contained in. The availability of school report card data varies by state: Illinois (2010–2019), Indiana (2005–2019), and Wisconsin (2011–2013 and 2015–2018). The regression includes only years in our study period, 2011–2018.

Table A4: AIC and BIC across models of location-utility on instrumented air quality

Distance function	Distance bands	Knots	AIC	BIC	AIC rank	BIC rank
exponential	2	3	903060.5	903101.6	1	1
euclidean	2	3	903061.9	903103	2	2
ihs	2	3	903062.6	903103.7	3	3
log	2	3	903062.6	903103.7	4	4
exponential	6	5	903065.6	903127.2	7	5
exponential	4	5	903065.6	903127.2	8	6
exponential	5	5	903065.6	903127.2	6	7
exponential	3	3	903068.1	903129.7	14	8
exponential	4	4	903080.4	903131.7	35	9
exponential	6	4	903080.4	903131.7	34	10
exponential	5	4	903080.4	903131.7	33	11
log	2	5	903070.6	903132.2	20	12
ihs	2	5	903070.8	903132.3	21	13
log	2	4	903070.8	903132.4	22	14
ihs	2	4	903071	903132.6	23	15
euclidean	2	4	903072.3	903133.9	26	16
euclidean	4	4	903065.6	903137.4	5	17
log	4	4	903065.6	903137.5	9	18
ihs	4	4	903065.6	903137.5	10	19
log	3	4	903066.2	903138.1	12	20
ihs	3	4	903066.2	903138.1	11	21
euclidean	3	4	903066.2	903138.1	13	22
log	6	4	903068.4	903140.3	15	23
ihs	6	4	903068.4	903140.3	16	24
euclidean	6	4	903070	903141.9	17	25
log	5	4	903070.2	903142.1	18	26
ihs	5	4	903070.3	903142.1	19	27
euclidean	5	4	903071.7	903143.6	24	28
euclidean	2	5	903072.2	903144	25	29
exponential	2	4	903082.4	903144	36	30
log	6	3	903073.4	903145.3	28	31
ihs	6	3	903073.4	903145.3	27	32
log	4	3	903073.9	903145.8	29	33
ihs	4	3	903073.9	903145.8	30	34
euclidean	6	3	903074.4	903146.3	31	35
ihs	3	3	903086.3	903147.9	40	36
euclidean	4	3	903076.1	903148	32	37
log	3	3	903086.6	903148.2	41	38
log	5	3	903084.5	903156.4	37	39
ihs	5	3	903084.5	903156.4	38	40
euclidean	5	3	903084.6	903156.4	39	41
euclidean	3	3	903099.4	903161	42	42
euclidean	6	5	903123.5	903195.4	43	43
exponential	5	3	903127	903198.9	44	44
ihs	5	5	903127	903198.9	45	45
ihs	3	5	903129.5	903201.3	46	46
log	3	5	903130.8	903202.6	47	47
log	5	5	903131.3	903203.1	48	48
exponential	3	5	903152.5	903224.4	49	49
exponential	3	4	903182.9	903254.8	50	50
log	6	5	903183.6	903255.4	51	51
exponential	6	3	903203.4	903275.3	53	52
ihs	6	5	903203.4	903275.3	52	53
exponential	4	3	903300.4	903372.3	54	54
ihs	4	5	903300.4	903372.3	55	55
log	4	5	903310.4	903382.3	56	56
exponential	2	5	903353.4	903425.3	57	57
euclidean	5	5	903682.7	903754.5	58	58
euclidean	3	5	903826.7	903898.6	59	59
euclidean	4	5	912656	912727.8	60	60

Table A5: Amenities on (quadratic) ambient air quality IV: fracking-predicted $PM_{2.5}$

	(1)	(2)	(3)	(4)	(5)
	Log rent	Arrest	Attendence	Eduation spend	Graduation
Ambient $PM_{2.5}$	-0.0515***	-1211.6	-6.343***	3.987	-17.97***
	(-2.902)	(-0.750)	(-11.08)	(0.738)	(-4.798)
Ambient $PM_{2.5}$ sq.	0.0105***	109.0	0.133***	-0.234	0.383
	(9.916)	(0.844)	(3.854)	(-0.539)	(1.566)
Zip	Yes				
Tract		Yes	Yes	Yes	Yes
Year	Yes	Yes	Yes	Yes	Yes
Property attributes	Yes				
Observations	6586547	21336	18291	22100	15291
R-squared	0.246	-4.939	-2.888	-0.188	-0.187

NOTES: T-stats are shown in parenthesis. $^{*}p < 0.1;^{**}p < 0.05;^{***}p < 0.001$. Rental property attributes include binary indicators for the availability of on street parking, off street parking, and garage, pool, fitness center, as well as the number of bedrooms and whether pets are allowed.

D Appendix: Alternative instrument for air quality

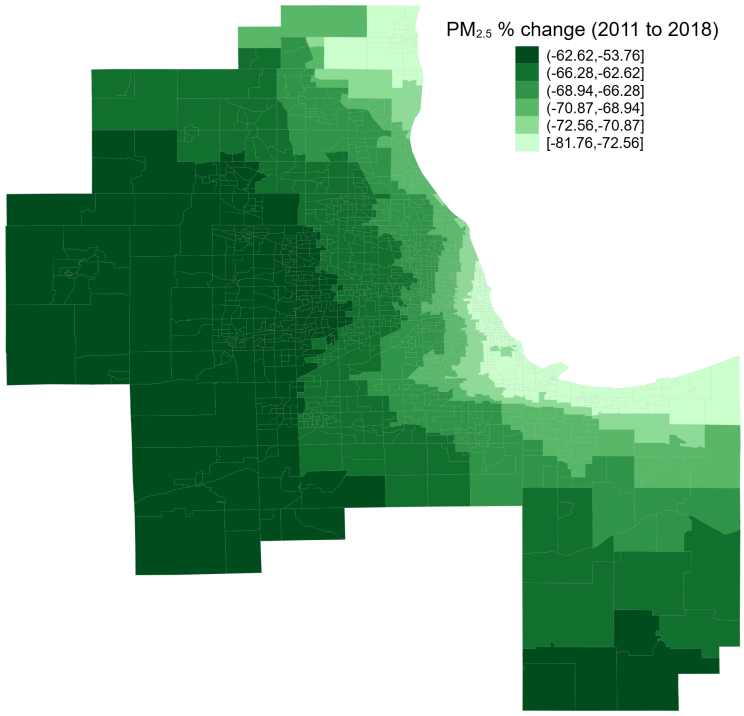
In this section, we discuss another plausibly exogenous source of air quality changes, $PM_{2.5}$ generated by emissions from electricity generating units outside of the Chicago CBSA. To satisfy the exclusion restriction in this setting, it must be the case that time-varying $PM_{2.5}$ generated from emissions from any particular generating unit are unrelated to time-varying components of the error term in equation (13). Since our pollution transport matrix is time invariant, and equation (13) includes tract fixed effects, the exclusion restriction can be discussed in terms of emissions from power plants and their relationship with time-varying components of the error term in equation (13).

If our estimating equation were at the county or state level, it may be plausible that time-varying components of location utility in the error term impact both utility and electricity demand. Local economic growth that adds retail stores could improve local utility while increasing emissions from generating units that increase production to meet this demand. In this setting, however, even this issue would be somewhat mitigated by the fact that economic growth is not likely to systematically increase emissions from upwind as opposed to downwind facilities. However, this type of channel is not likely relevant for an estimation at the census tract level. At this small geographic scale, it is unlikely that local factors that affect the utility of the tract are systematically correlated with time-varying factors that affect emissions in upwind facilities. However, increasing or decreasing emissions from generating units in the Chicago CBSA would be more likely to have very local effects, for example, from heavier pollutants with smaller dispersal patterns, and thus for this instrument we remove the two electricity generating units located in the CBSA.

We rerun our analysis in this main text with electricity generated $PM_{2.5}$ as our instrument, henceforth, our electricity instrument. The construction of this instrument follows the procedure in Hernandez-Cortes, Meng and Weber (2023), which describes the data and methods to construct $PM_{2.5}$ concentrations attributable to emissions from electricity generating units. Figure A11 shows air quality changes in Chicago CBSA from 2018 compared to 2011 with our instrument generated with electricity $PM_{2.5}$. Comparing this Figure with Figure A9, we see that the electricity instrument generates a more systematic pattern of improvements, increasing from the South-West to the North-East of Chicago. Also, predicted improvements in percent change are larger.

Figure A12 replicates the results presented in Figure 5 with this instrument. Comparing these two Figures, the results with electricity instrument are broadly the same as with the fracking instrument. In both Figures the changes in racial pollution gaps are lower and/or reversed in the sorting framework compared to the non-sorting framework. Both Figures' panel (A) show reductions in Black-white racial welfare gaps. Both Figures' panel (B) show reductions in Hispanic racials welfare gap in some and not all policies.

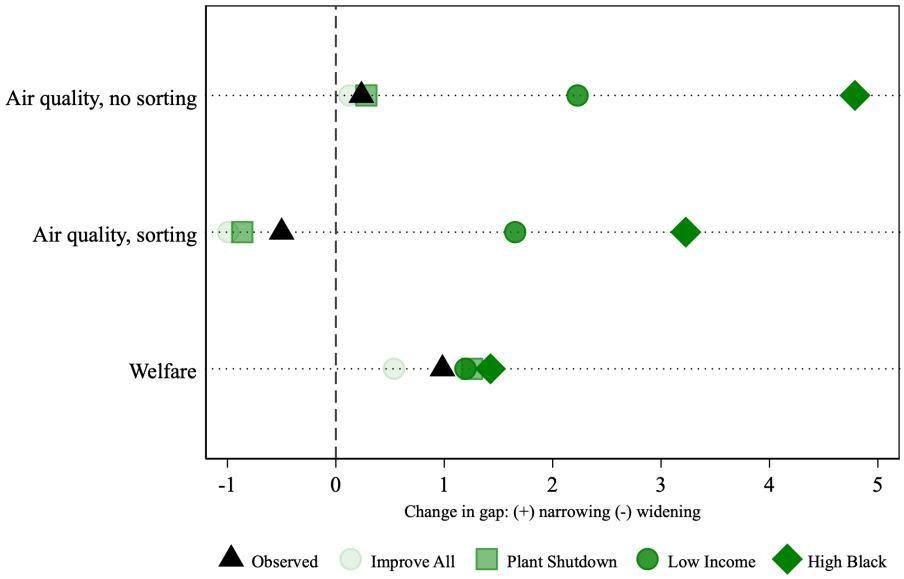
Figure A11: Changes in predicted $PM_{2.5}$ from electricity generation



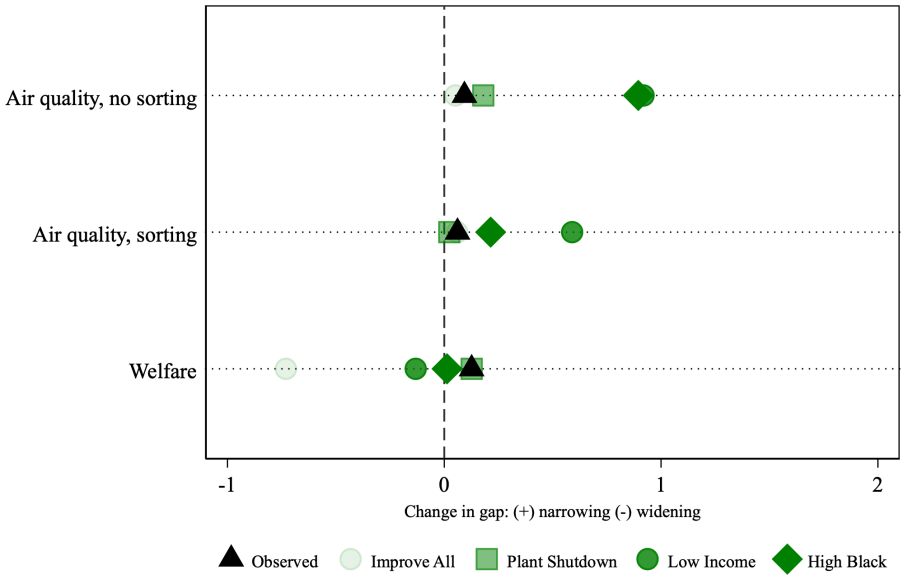
NOTES: This Figure plots changes in ambient $PM_{2.5}$ from 2018 to 2011 using the annual $PM_{2.5}$ predicted from our electricity $PM_{2.5}$ instrument.

Figure A12: Change in racial pollution gap: electricity instrument for $PM_{2.5}$

(A) Black—white



(B) Hispanic—white



NOTES: The rows of each sub figure show the estimates of Δx, $\Delta \widetilde{x}$, and ΔW from equation (1), (1"), and (1"') with the same approach as in the main text except here we use the electricity pollution instrument presented in this appendix. Panel (A) shows shows the metric comparing Black to white renters, and panel (B) shows the metric comparing Hispanic to white renters.

E Appendix: Long difference version of sorting model

We estimate an alternative version of the sorting model that relaxes the assumption that location utilities re-equilibrate annually from amenity changes. In this version of the model, we assume that it takes the full study period to reach a new equilibrium, and estimate the model based on location choices and air quality in 2011 and 2018. We call this the long difference version of the sorting model. The long difference model estimates how changes in air quality at the end of the study period compared to the beginning change residential renter location decisions and welfare by only using data at the beginning and end of the study period.

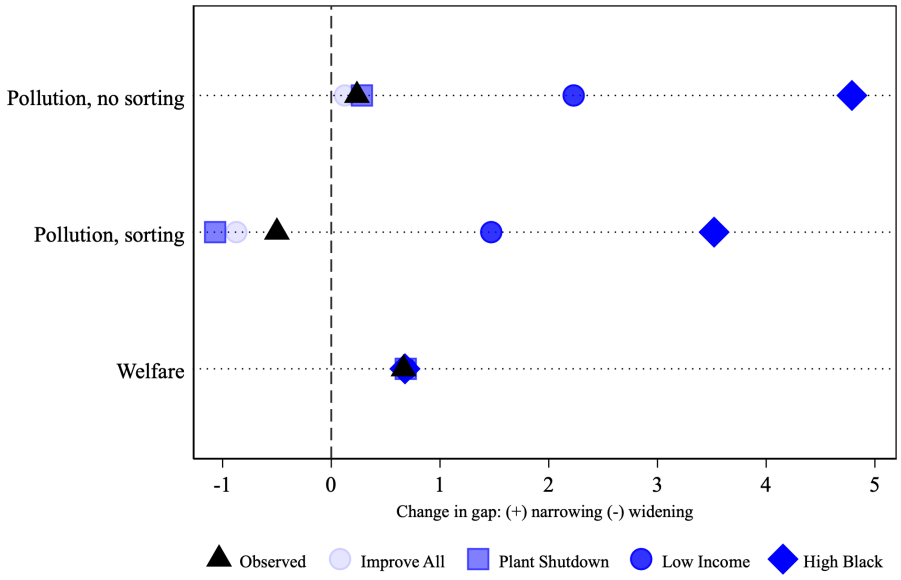
In the long-difference model, renters are coded as movers in 2011 if they changed census tracts in 2011 compared to 2010. Movers in 2018 are renters who change tracts in 2018 compared to 2011. This empirical choice introduces a difference in the mover coding at the end of the study period compared to the beginning. An alternative would be to code 2011 movers as anyone who changed tracts in 2011 compared to 7 years prior. We avoid doing this for two reasons. One, our goal with this exercise is to generate a comparable set of results with the main annual version of the model, and so in that respect we do not want to introduce new years outside the study period included in the annual model. Two, the air quality improvements, and those explained by our instrument, are more pronounced during our study period. This mover coding choice impacts our estimate of time invariant moving costs in the long difference sorting model. To the extent that this generates an undercount of movers in 2011 compared to movers in 2018, that would bias moving cost estimates upward in a long difference framework. Note, moving costs across the annual and long difference models should not be compared as each model includes its own unique normalization of location utilities.

Our estimates of changes in the racial welfare and pollution gaps in the long difference version of the model are presented in Figure A13. The analogous results with our annual sorting model are shown in Figure 5. Comparing the Figures' panel (A) shows that the takeaways from the long distance model are broadly the same as in the annual model. In both models, changes in the Black-white pollution gap are larger in a no-sorting framework compared to a sorting framework. In both models, all policies decrease Black-white welfare gaps. One difference in the long difference model is that the variation in the policies' effects on the welfare racial gap is attenuated compared to the annual model. Comparing the Figures' panel (B), we seethat the long difference model predicts a reduction in racial welfare gap between Hispanic and white renters in all policies, whereas the annual model predicts this gap decreases for some but not all policies. As with the annual model, the long difference model shows reduction in pollution gaps in a no sorting framework, which are smaller and or do not hold for pollution in the sorting framework.

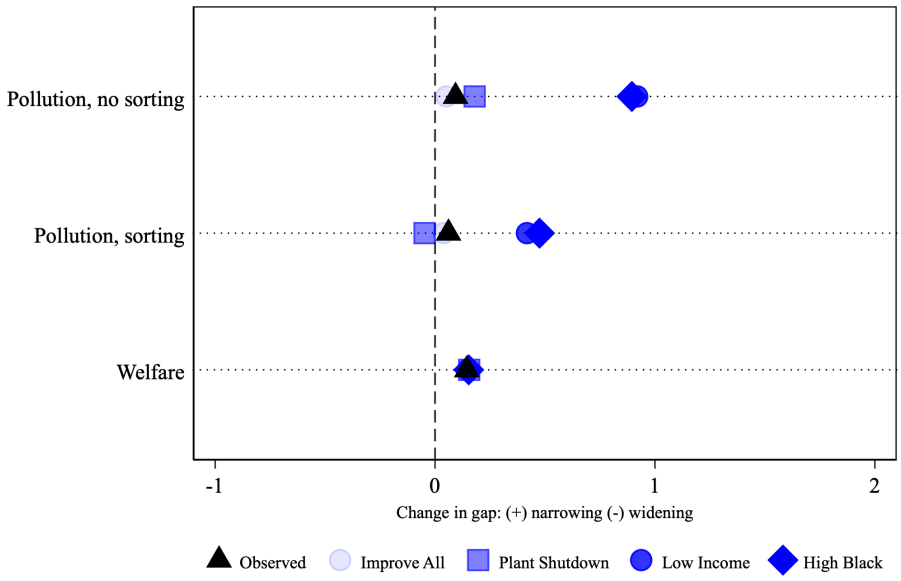
Our annual model is our preferred specification, as it leverages annual variation in location choices and air quality, and it more closely approximates location choices for renters, for which annual leases are common.

Figure A13: Change in racial pollution gap: long difference sorting model

(A) Black—white



(B) Hispanic—white



NOTES: The rows of each sub figure show the estimates of Δx, $\Delta \widetilde{x}$, and ΔW from equation (1), (1"), and (1"') using a long difference version of the sorting model. Panel (A) shows shows the metric comparing Black to white renters, and panel (B) shows the metric comparing Hispanic to white renters.